Recent advances in nanomaterials for the detection of mycobacterium tuberculosis (Review)

JIANMENG ZHU[1], HONGQIN WANG[1] and LILI CHEN[2]

[1]Clinical Laboratory of Chun'an First People's Hospital, Zhejiang Provincial People's Hospital Chun'an Branch, Affiliated Chun'an Hospital of Hangzhou Medical College, Hangzhou, Zhejiang 311700, P.R. China; [2]Orthopedics of Chun'an First People's Hospital, Zhejiang Provincial People's Hospital Chun'an Branch, Affiliated Chun'an Hospital of Hangzhou Medical College, Hangzhou, Zhejiang 311700, P.R. China

Received August 27, 2024; Accepted December 12, 2024

DOI: 10.3892/ijmm.2024.5477

Abstract. The world's leading infectious disease killer tuberculosis (TB) has >10 million new cases and ~1.5 million mortalities yearly. Effective TB control and management depends on accurate and timely diagnosis to improve treatment, curb transmission and reduce the burden on the medical system. Current clinical diagnostic methods for tuberculosis face the shortcomings of limited accuracy and sensitivity, time consumption and high cost of equipment and reagents. Nanomaterials have markedly enhanced the sensitivity, specificity and speed of TB detection in recent years, owing to their distinctive physical and chemical features. They offer several biomolecular binding sites, enabling the simultaneous identification of multiple TB biomarkers. Biosensors utilizing nanomaterials are often compact, user-friendly and well-suited for detecting TB on location and in settings with limited resources. The present review aimed to review the advances that have occurred during the last five years in the application of nanomaterials for TB diagnostics, focusing on their detection capabilities, structures, working principles and the significance of key nanomaterials. The current review addressed the limitations and challenges of nanomaterials-based TB diagnostics, along with potential solutions.

Correspondence to: Professor Lili Chen,Orthopedics of Chun'an First People's Hospital, Zhejiang Provincial People's Hospital Chun'an Branch, Affiliated Chun'an Hospital of Hangzhou Medical College, 1869 Huanhu North Road, Chunan, Hangzhou, Zhejiang 311700, P.R. China
E-mail: lilichen_hz@126.com

Abbreviations: MTB, Mycobacterium tuberculosis; TB, tuberculosis; Au, gold; Ag, silver; ssDNA, single-stranded probe DNA; SPR, surface plasmon resonance; PNAs, peptide nucleic acids; acpcPNA, PNA with a positively charged lysine modification at its C-terminus; MNPs, magnetic nanoparticles; GMR, giant magnetoresistance; ESAT-6, early secreted antigenic target-6; MPT64, MTB 64 protein; QDs, quantum dots; SiNPs, silica nanoparticles; CFP10, culture filtrate antigen, 10 kDa; FRET, fluorescence resonance energy transfer; QDs-DNA, carboxyl-modified CdTe QDs to label single-stranded DNA; NB, nanobeacon; MNAzyme, multicomponent nuclease; CoTCPP, cobalt-metalized tetrakis(4-carboxyphenyl) porphyrin; nanoCoTPyP, nanocobalt 5,10,15,20-tetra(4-pyridyl)-21H,23H porphine; rGO, reduced graphene oxide; PNE, polynorepinephrine; PDA, polydopamine; PADs, paper-based analytical devices; GCOOH, carboxyl graphene; FET, field-effect transistor; GFETs, graphene-based field-effect transistors; SWCNTs, single-walled carbon nanotubes; Ab85B, anti-MTB antigen 85B antibody; Ag85B, MTB-secreted antigen 85B; 1,5-DAN, 1,5-diaminonaphthalene; FNDs, fluorescent nanodiamonds; EDC, 1-Ethyl-3-(3-dimethylaminopropyl) carbodiimide; NHS, N-hydroxysuccinimide

Key words: tuberculosis, nanomaterials, diagnostics, biosensors

Contents

1. Introduction

Mycobacterium tuberculosis (MTB) infection causes tuberculosis (TB), which affects 25% of the world's population. In 2022, the World Health Organization reported 10.6 million new TB infections, 133 per 100,000 persons and 1.3 million mortalities (1). TB is the second most deadly infectious disease worldwide, surpassed only by COVID-19, with its mortality rate nearly double that of HIV/AIDS (2). Early and accurate TB diagnosis is crucial for its control and management (3). Early discovery improves therapy, limiting illness progression and serious consequences (4). Accurate identification of TB cases can reduce the spread of MTB, especially in densely populated and resource-limited areas, thereby reducing pressure on the healthcare system (5).

Immunological, radiographic and bacteriological methods are used to diagnose TB (6). The tuberculin skin test and INF-γ release assay are simple immunological

assays that detect TB within 72 h. However, the window time of the disease, the immune system and experimental methods can cause false positives and negatives (7). Chest X-rays and computerized tomography scans can detect lung abnormalities and track illness progression, but they are less sensitive and specific and cannot distinguish TB from other lung infectious disorders (8,9). Antacid smear microscopy and sputum culture are the main bacterial tests; however, smear microscopy has just 30% sensitivity and mycobacterial culture, the gold standard, takes 2 weeks to provide positive results, during which MTB will spread in the population (10,11). Automated Nucleic Acid Amplification (PCR) Assay System (GeneXpert) can detect MTB and rifampicin resistance in 2 h (12); however, due to the expensive cost of instruments and reagents and the strict environmental requirements of the assay, GeneXpert is challenging to apply in distant and impoverished locations and its sensitivity is still limited for sputum specimens with low bacterial loads (13). Thus, rapid, cost-effective, precise and sensitive TB diagnostic methods are needed.

Nanomaterials have advanced TB diagnostics in recent years (14). Their high surface area-to-volume ratio provides more reaction sites, greatly enhancing detection sensitivity and enabling accurate TB detection even at low bacterial loads (15). Nanomaterial-based detection technologies frequently yield fast outcomes (16). For example, colorimetric reactions or electrochemical biosensors based on gold (Au) and silver (Ag) nanoparticles (NPs) markedly reduce the time required for conventional detection methods (17,18). Nanomaterials can bind to multiple molecules, allowing simultaneous detection of various TB biomarkers (19). Such multifunctional platforms provide comprehensive diagnostic information, enhancing accuracy and practicality (20). For example, AuNPs allow for the attachment of multiple antibodies or oligonucleotides, which can specifically bind to different TB biomarkers (21). Similarly, quantum dots (QDs) can be conjugated with multiple oligonucleotide probes that are complementary to different segments of the TB genetic material (22). This allows for the simultaneous detection of multiple TB genetic markers. The ability to detect multiple biomarkers simultaneously is particularly beneficial in the early stages of TB infection, where the bacterial load may be low and in differentiating TB from other respiratory diseases that have similar symptoms (23). It also aids in the rapid identification of drug-resistant TB strains, which is vital for initiating appropriate treatment strategies (24,25).

Due to the efficiency and simplicity of nanotechnology, diagnostic devices based on nanomaterials are typically compact and easy to operate, making them suitable for on-site testing and resource-limited settings (26). Fig. 1 presents the nanomaterials and corresponding biosensors for TB diagnosis. The current article reviewed the latest research advances in TB diagnostics using nanomaterials, including their mechanisms and functions and analyzes the structure and performance of various novel nano biosensors. The limitations and challenges of nanomaterials in TB diagnosis are also discussed, along with strategies to overcome them. The present review aims to provide researchers with insights for developing safe, rapid and effective TB diagnostic methods.

2. Metal nanomaterials-based diagnostics for TB

Metal nanoparticles improve TB diagnosis by overcoming some traditional drawbacks. Table I presents recent advances in metal nanomaterials-based diagnostics for TB. Due to their optical, electronic and magnetic characteristics, they can be modified with various ligands and detect TB biomarkers at low concentrations (13,27). Moreover, they can be designed to be portable and user-friendly for convenient use at the medical treatment site. This allows for the adoption of decentralized testing in areas with limited resources, making diagnostic assays potentially more affordable (28).

AuNPs-based TB detection. AuNPs can attach multiple diagnostic probe molecules due to their high surface-to-volume ratio (44). They can be used for long-term diagnostics since they are chemically stable and air- and water-resistant (18). The first reported application of AuNPs in TB diagnosis was a colorimetric assay developed by Gupta *et al* (45). In that study, oligonucleotides of the Mycobacterium tuberculosis RNA polymerase subunit gene sequence were first extracted and then combined with AuNPs and, at a wavelength of 526 nm, the gold nanoprobe solution stayed pink in the presence of the complementary DNA. By contrast, the solution turned purple without the complementary DNA. The assay takes only 15 min per test, with minimal contamination, as it is performed in a separate tube and allows visualization of the results. Follow-up studies showed that this approach detected TB more precisely and sensitively when compared with the automated liquid culture system and semi-nested PCR (46,47).

AuNP aggregation via salt, such as NaCl and $MgSO_4$, is the most widely used AuNP-based colorimetric method for TB DNA detection. The amount of TB DNA to be detected is inversely proportional to the salt concentration required to cause AuNPs to aggregate (16,27). However, this may lead to false negative signals when the TB DNA content is low, as the salt concentration required to detect AuNP aggregation is very high. Thus, Tripathi *et al* (32) relied on ethanol-induced AuNP aggregation to detect TB DNA. Ethanol affected the hydrophobic and electrostatic interactions of AuNPs with DNA, generating dipole-dipole interactions that led to AuNP aggregation. As shown in Fig. 2, a 4 μl 100% ethanol addition to the AuNPs-TB DNA complex could cause aggregation. Without TB DNA, AuNP suspensions did not aggregate despite the introduction of 8 μl of 100% ethanol. This method sensitively detects MTB DNA at ~340 fM levels, amplified with a 0.125 ng ml^{-1} template and produces results in <3 min. Contrary to salt-based AuNP aggregation methods, the researchers claimed their method is sensitive and reliable for early TB identification. This simple, easy-to-use approach does not require AuNP or oligonucleotide modification or expensive equipment, making it favorable in resource-poor settings.

The local electric field enhancement effect induced by surface plasmon resonance (SPR) can enhance the optical activity near the surface of metal nanoparticles, such as surface-enhanced Raman scattering and fluorescence enhancement. The plasma-enhanced effect of AuNPs has several applications in fields such as biomarkers, sensors, photocatalysis and optoelectronics (48,49). Plasma coupling

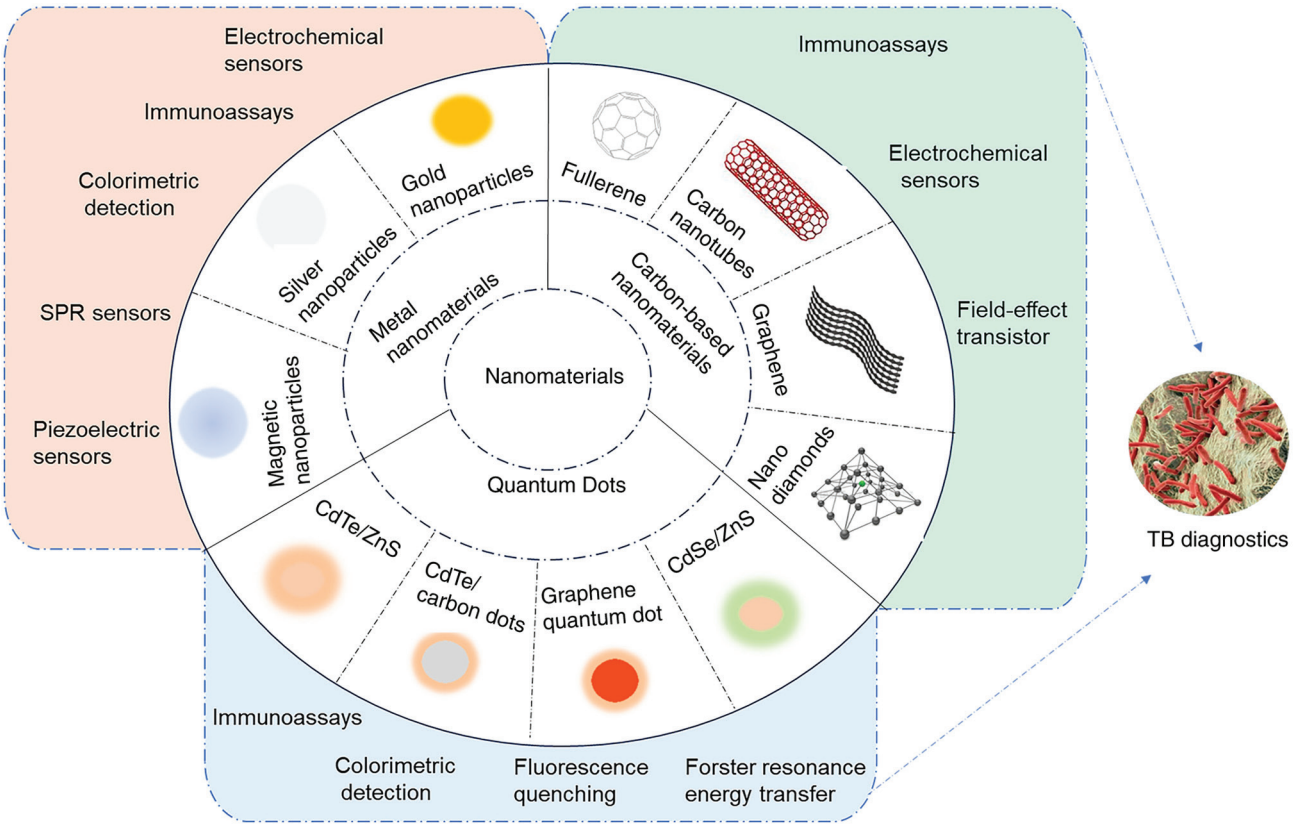

Figure 1. Nanomaterial-based biosensing strategies for TB diagnosis. TB, tuberculosis; SPR, surface plasmon resonance.

is related to the size, shape, structure and spatial arrangement of NPs (50). Research in this area can help to optimize biosensor structures. Prabowo *et al* (39) studied the effect of AuNP shapes on plasmonic enhancement for DNA detection. They bound TB's designed single-stranded probe DNA (ssDNA) with gold nano-urchins and nanorods. Then, both mixtures were adsorbent onto a graphene-coated SPR sensor due to the π-π interactions. During the construction of the SPR sensor, annealing the Au layer increased the sensor's graphene coverage and DNA probe load. In experimental plasmonic activity comparison, gold nano-urchins showed the best amplification, detecting DNA hybridization at fM levels. They conclude that gold nano-urchin-assisted DNA detection offers the possibility of early screening for TB using portable sensors.

Due to their affordable cost, simple structure and easy operation, piezoelectric sensors are becoming a TB detection research hotspot (51). A piezoelectric sensor generates electricity from pressure, acceleration and force. Quartz, Rochelle salt and some ceramics generate an electrical charge when subject to mechanical stress, a phenomenon known as the piezoelectric effect (52). Exploiting the special physical and chemical properties of Au at the nanoscale, AuNPs can markedly enhance the performance of piezoelectric sensors for detecting MTB (53). Zhang *et al* (37) developed a novel piezoelectric sensor based on AuNPs-mediated enzyme-assisted signal amplification for TB diagnosis (Fig. 3A). The biomarker was the 16S rDNA variable region of TB. AuNPs were coupled to the hybridized detecting probe and grown in $HAuCl_4$ and NADH solutions to transmit electricity between electrode gaps (Fig. 3B). The piezoelectric system detects TB rapidly and sensitively thanks to AuNPs-mediated signal amplification. The process is simple, fast and suited for developing compact portable equipment.

AgNPs-based TB detection. AgNPs, like AuNPs, are chemically stable, electrically conductive and can possess catalytic activity. Their electron transfer efficiency is superior to that of AuNPs, which have more prominent extinction bands (18). Recent advances have seen the use of charge-neutral peptide nucleic acids (PNAs) as hybridization agents in AgNP-based colorimetric DNA assays, enhancing the process by causing nanoparticles to cluster more rapidly in solution without immobilization, thus boosting DNA hybridization effectiveness. Teengam *et al* (54) developed a colorimetric DNA detection sensor based on PNA-induced AgNP aggregation (Fig. 4A). They designed a detection probe from PNA with a positively charged lysine modification at its C-terminus (acpcPNA), leading to the aggregation of negatively charged AgNPs and a subsequent swift shift in color. This sensor effectively detected TB oligonucleotides, demonstrating a low detection limit of 1.27 nM, showcasing fast, selective and sensitive DNA detection capability.

Conventional methods for producing AgNPs typically involve the use of reducing agents such as sodium citrate, $NaBH_4$ and hydrazine. While effective in controlling nanoparticle size, these agents pose significant environmental risks (55,56), prompting the pursuit of greener alternatives. Tai *et al* (40) devised a method to synthesize AgNPs using oil palm lignin, which is rich in phenolic hydroxyl groups and

Table I. Recent advances in metal nanomaterials-based diagnostics for tuberculosis.

First author/s, year	Nanomaterials	Detection assays	Target	LOD	Detection Time/ Sample type	(Refs.)
Seele *et al*, 2023	AuNPs	Lateral flow Immunoassays	CFP-10/ ESAT-6	7.69/0.063 ng/ml	15 min/Spiked sample	(29)
Kamra *et al*, 2023	MB-AuNP	Immuno-PCR assay	MPT-64	1 fg/ml	NA/Clinical sample	(30)
Dahiya *et al*, 2023	MB-AuNP	Immuno-PCR assay	MPT-64/ CFP-10	9.9 ng/ml	NA/Clinical sample	(31)
Tripathi *et al*, 2023	AuNPs	Colorimetric detection	MTB DNA	0.125 ng/ml	3 min/Amplified sample	(32)
Huang *et al*, 2023	MXene/C_{60}NPs/ Au@Pt	Electrochemical sensor	ESAT-6	2.88 fg/ml	NA/Clinical sample	(33)
Patnaik *et al*, 2024	AgNPs	AgNP aggregation	MTB DNA	4 bacilli	20-25 min/ Amplified sample	(34)
Pei *et al*, 2022	AuNPs	Dark-field imaging	MTB DNA	10 fM	1 h/Spiked sample	(35)
León-Janampa *et al*, 2022	MNP@Si@ab	sELISA	MTB antigens	0.15 ng/μl (38 kDa, MoeX, Ag85B) 0.31 ng/μl (MPT64, MTC28) 1.25 ng/μl (CFP10, ESAT6)	4 h/Clinical sample	(36)
Zhang *et al*, 2022	AuNPs	Piezoelectric sensor	16 S rDNA	30 CFU/ml	3 h/Amplified sample	(37)
Xie *et al*, 2021	NG@Zr-MOF-on-Ce-MOF@Tb	Electrochemical aptasensor	ESAT-6	12 fg/ml	NA/Clinical sample	(38)
Prabowo *et al*, 2021	AuNP-ssDNA	SPR sensor	MTB DNA	24.5 fM	NA/NA	(39)
Tai *et al*, 2021	LSG-NF-AgNP	Electrochemical sensor	MTB DNA	10^{-15} M	NA/Amplified sample	(40)
Azmi *et al*, 2021	Fe_3O_4/Au	Sandwich-type immunosensor	CFP10-ESAT6	1.5 ng/ml	2 h/clinical sample	(41)
Gupta *et al*, 2021	MNPs	Giant magneto-resistance	ESAT-6	1 pg/ml	NA/Clinical sample	(42)
León-Janampa *et al*, 2020	MNP@Si@NH_2	sELISA	Hsp16.3	0.9 pmol	NA/purified sample	(43)

CFP-10, CFP10, culture filtrate antigen, 10 kDa; ESAT-6, early secreted antigenic target-6; MPT64, MTB 64 protein; LOD, limit of detection; NA, not available; MB-AuNP, magnetic bead-coupled gold nanoparticle; MOF, metal-organic framework; NG, nitrogen-doped graphene; Tb, electroactive toluidine blue; SPR, surface plasmon resonance; LSG-NF, graphene nanofiber laser biosensor; MNPs, magnetic nanoparticles; ab, polyclonal antibodies; sELISA, sandwich enzyme-linked immunosorbent assay.

offers an environmentally friendly and cost-efficient solution for AgNP production. These lignin-coated AgNPs were subsequently bonded to laser-etched graphene nanofibers, enabling the direct linkage of single-stranded DNA to form a TB bioelectrode. To assess the performance of the sensor, they analyzed the ability of DNA samples attached to AgNPs to bind to the target DNA by selective hybridization and mismatch assessment. Electrochemical impedance spectroscopy further substantiated the ability of the sensor to detect concentrations as low as 1 fM, achieving a detection limit of 10^{-15}M based on

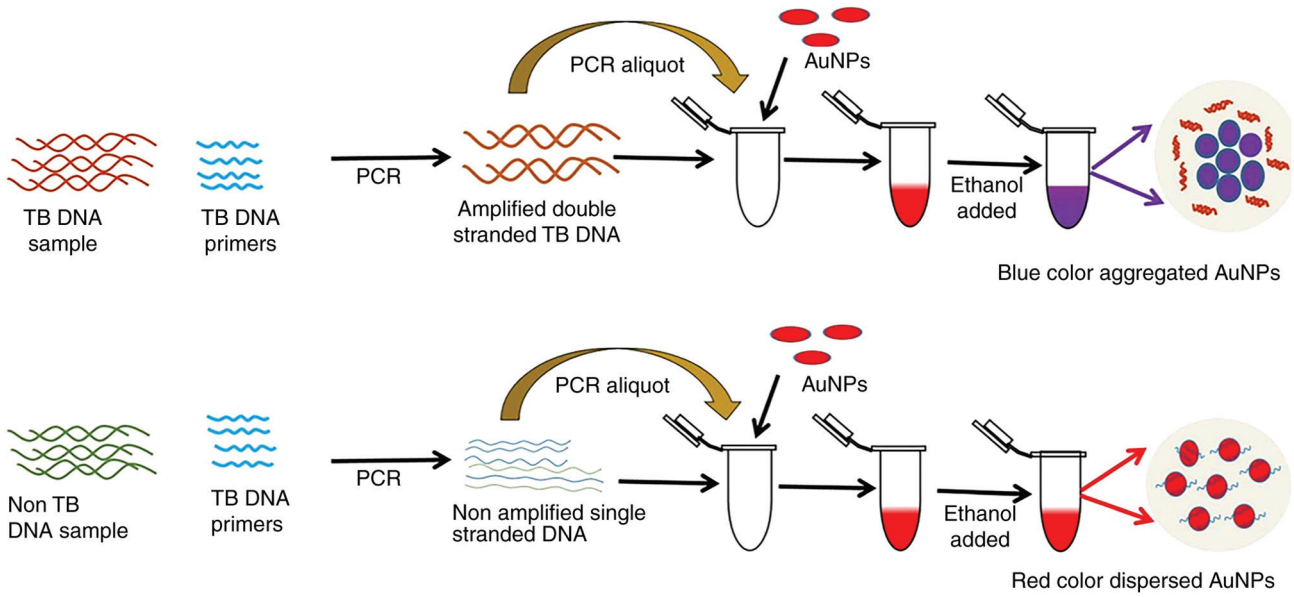

Figure 2. AuNPs-based colorimetric detection of TB DNA Schematic diagram: Two PCR tubes were made using TB primers and PCR mix. The TB DNA template was placed in one tube and the other tube without the TB DNA template. After PCR, AuNPs and ethanol were added. The tube without the DNA template stayed red, while the tube with TB DNA turned purple. Reproduced from (32), Copyright (2023), with permission from Royal Society of Chemistry. AuNPs, gold nanoparticles; TB, tuberculosis.

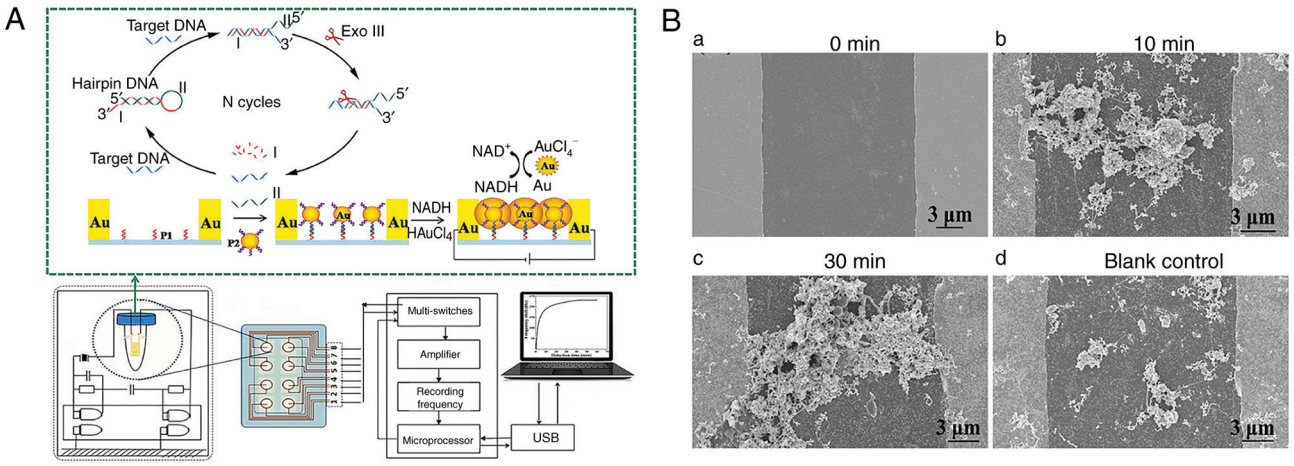

Figure 3. Procedure of piezoelectric sensor based on AuNPs-mediated enzyme-assisted signal amplification. (A) SEM images of electrodes promoting the growth of AuNPs in $HAuCl_4$ and NADH solutions containing target DNA and Exo III for (Ba) 0 min, (b) 10 min, (c) 30 min and (d) blank control. Reproduced from (37), Copyright (2022), with permission from Elsevier. AuNPs, gold nanoparticles.

a signal-to-noise ratio (S/N=3:1) with a signal-to-noise ratio of 3:1. The researchers highlighted that this TB detection method is sensitive and ecologically friendly.

Magnetic nanoparticles (MNPs)-based TB detection. MNPs are generally composed of iron, nickel, cobalt and oxides. MNPs feature a high surface-to-volume ratio, excellent dispersibility and strong interactions with biological molecules (57). Gupta *et al* (42) developed a giant magnetoresistance (GMR) biosensor to detect TB-specific early secreted antigenic target-6 (ESAT-6) protein. This GMR biosensing assay labels monoclonal antibodies against ESAT-6 antigen with MNPs. In the presence of ESAT-6, MNPs bind to the GMR sensor proportionally to protein concentration, altering its electrical resistance. Simulations of the GMR biosensor have shown that it can detect ESAT-6 at pg/ml levels. Cheon *et al* (58) developed a colorimetric biosensing system to detect MTB 64 protein (MPT64) using nucleic acid aptamer-modified MNPs. The aptamer on the surface of the MNP initially inhibits its catalase activity. Upon binding with MPT64 in the sample, the aptamer releases, thereby restoring the enzyme activity of the MNP. TB can subsequently be detected within 70 min by measuring the enzyme-substrate fluorescence spectra.

Mohd *et al* (41) developed a portable sandwich-based electrochemical immunoassay device for clinical sputum TB detection (Fig. 4B). They used Fe_3O_4/Au MNPs to capture anti-culture filtrate antigen [CFP10 (10 kDa)-early secreted antigenic target-6 (ESAT6; 6kDa)] antibody, which is more stable than enzyme-conjugated antibodies. Magnetic Fe_3O_4 particles enhance the chemical stability and biocompatibility

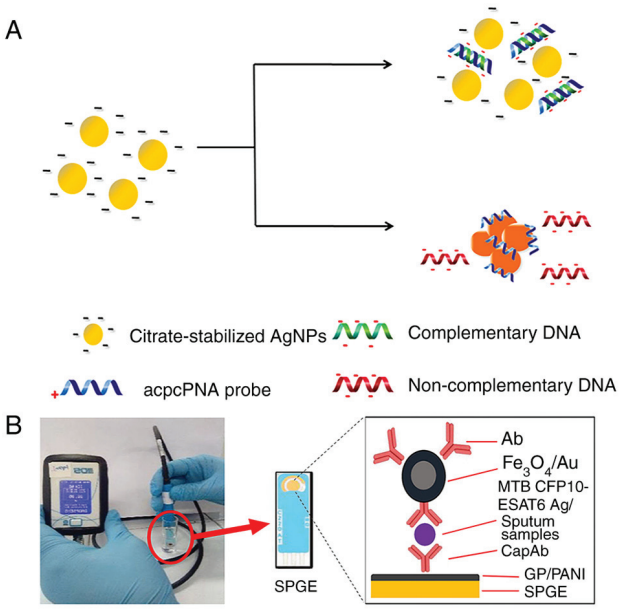

Figure 4. Procedure for acpcPNA-induced AgNP aggregation. (A) AgNPs were initially well dispersed by the negatively charged electrostatic repulsion. Positively charged acpcPNA shielded them from electrostatic repulsion, causing silver particles to aggregate and a color reaction to occur. When complementary DNA was present, the specific PNA-DNA interaction replaced the PNA-AgNPs interaction, forming negatively charged PNA-DNA double strands that depolymerized the nanoparticles. In the case of non-complementary DNA, the nanoparticles did not depolymerize and no color change occurred. Reproduced from (54), Copyright (2017), with permission through Creative Commons public use license from Teengam P *et al*, American Chemical Society. (B) Schematic of CFP10-ESAT6 detection using the portable electrochemical reader. Sputum sample analysis was performed locally with the modified SPGE (circled in red) and a portable reader. Following GP/PANI modification of SPGE, the CapAb was immobilized on its surface to capture the target antigen and the Ab-loaded Fe_3O_4/Au particle bound to the target and amplified the detection signal. Reproduced from (41), Copyright (2021), with permission from Springer Nature. acpcPNA, PNA with a positively charged lysine modification at its C-terminus; AuNPs, gold nanoparticles; PNA, peptide nucleic acid; CFP10, culture filtrate antigen, 10 kDa; ESAT-6, early secreted antigenic target-6; SPGE, screen-printed gold electrode; GP/PANI, graphene/polyaniline; CapAb, capture antibody; MTB, Mycobacterium tuberculosis.

of Au. Results revealed an excellent correlation in sensitivity (100%) and specificity (91.7%) compared with the gold standard culture method. León-Janampa *et al* (36) presented a colorimetric sandwich assay incorporating amino-silanized MNPs functionalized with anti-MTB polyclonal antibodies to detect TB in sputum. The biofunctionalized MNPs enhance antigen capture from biological materials, enabling multiple TB antigen detection and decreasing test time compared with traditional ELISA. This method can also evaluate TB markers in early TB cultures, urine and serum.

3. QDs-based TB diagnostics

QDs are nanoscale semiconductor particles with size-tunable fluorescence, meaning smaller dots emit blue light while larger ones emit red light (19). As fluorescent probes, QDs can mark MTB nucleic acid and are more photostable and less prone to photobleaching than organic dyes (59). The surface of QDs can be modified with various functional groups or nanomaterials to improve their solubility, stability and biocompatibility (60). Table II presents recent advances in quantum dots (QDs) based diagnostics for TB.

Bakhori *et al* (68) reported an electrochemical platform based on CdSe/ZnS QDs and silica nanoparticles (SiNPs) to detect TB-specific biomarkers (CFP10–ESAT6). They demonstrated that the active surface area of the CdSe/ZnS QD/SiNPs modified electrode was 4.14-fold higher than a bare electrode. Results indicated a linear calibration curve in the 40-100 ng/ml target concentration range, with a detection limit of $1.2x10^{-9}$ g/ml for CdSe/ZnS QD/SiNPs modified electrode and $1.5x10^{-10}$ g/ml for SiNPs modified electrode. These results indicated that the CdSe/ZnS QD-modified electrode has superior electrochemical behavior, which improves electron transfer between the electrode and the target.

In fluorescence resonance energy transfer (FRET)-based systems, QDs can provide energy and bind acceptors. When these probes attach to target nucleic acids such as MTB RNA or DNA, structural alterations influence energy transfer efficiency, resulting in quenching or fluorescence changes, allowing quantitative analysis (69,70). This QD quenching technology-based biosensor serves as a fast, sensitive and easy-to-use diagnostic tool (71). Liang *et al* (67) used carboxyl-modified CdTe QDs to label single-stranded DNA (QDs-DNA) as a fluorescence donor. In their approach, Cu-TCPP (a two-dimensional metal-organic framework) nanosheets were used as the fluorescence acceptor for QDs-DNA. QDs-DNA attached to Cu-TCPP, resulting in fluorescence quenching in the absence of targets. However, when the target nucleic acids were present, QDs-DNA formed with them a dsDNA complex, preserving strong fluorescence (Fig. 5A). The sensor exhibited a linear response from 0.05 to 1.0 nM and a 35 pM detection limit. This QD-based fluorescent technology for clinical sputum analysis achieved high sensitivity and specificity.

Hu *et al* (61) proposed a QD-nanobeacon (NB)-based colorimetric platform for TB diagnosis, where the QD-NB acted as a cleavable substrate and a signal indicator. As shown in Fig. 5B, they conducted recombinase polymerase amplification in the presence of the target DNA and chemically denatured the amplicon for DNA, followed by a multicomponent nuclease (MNAzyme) reaction. The MNAzyme identified the target DNA and hybridized with the QD-NB. Upon adding Mg^{2+}, the QD-NB was cleaved into two DNA fragments, triggering the release of green fluorescence due to the FRET effect of QDs. This QD-NB-based MNAzyme colorimetric assay achieved a detection limit of 2 copies/μl, cost ~$4 in reagents and took only 55 min to complete.

The primary inner filter effect (IFE) is the absorption of excitation light by various chromophores in solution or matrix, while the secondary inner filter effect refers to the absorption of emission radiation (72). He *et al* (62) found that cobalt-metalized tetrakis (4-carboxyphenyl) porphyrin (CoTCPP) could modulate the fluorescence emission and quenching of QDs through the inner filter effect. Thus, they developed a fluorescent probe based on CdTe QDs and CoTCPP nanosheets to analyze methyl nicotinate in vapor samples of MTB (Fig. 6). CoTCPP and QDs cannot become close enough to access FRET due to electrostatic repulsion. By contrast, the IFE affects QD fluorescence quenching. They used red-emitting QDs as fluorescent signal switches whose fluorescent are quenched by CoTCPP but restored by methyl

Table II. Recent advances in quantum dots based diagnostics for tuberculosis.

First author/s, year	Nanomaterials	Detection assays	Target	LOD	Detection time	(Refs.)
Hu *et al*, 2023	CdTe:Zn^{2+} QD-NB	Colorimetric assays	MTB DNA	2 copies/μl	55 min	(61)
He *et al*, 2022	CdTe QD/CoTCPP	Fluorescence quenching	Methyl nicotinate	0.59 μM	4 min	(62)
Hu *et al*, 2022	Double CdTe QDs/ nanoCoTPyP	Fluorescence quenching	rpoB531/ katG315	24/20 pM	95 min	(63)
Kabwe *et al*, 2022	MA-CdSe/ZnS QDs	Visual paper-based lateral flow	Anti-MA antibodies	NA	NA	(64)
Shi *et al*, 2024	CdTe QD/carbon dots	Fluorescence quantification strategy	IFN-γ/IP-10	0.3/0.5 ag/ml	8 h	(65)
Kabwe *et al*, 2022	MA-GQDs	Lateral flow tests	Anti-MA antibodies	NA	NA	(66)
Liang *et al*, 2021	CdTe QDs/ Cu-TCPP	FRET	IS6110	35 pM	50 min	(67)

LOD, limit of detection; MTB, Mycobacterium tuberculosis; QD-NB, quantum dot-based nanobeacon; NA, not available; CoTCPP, cobalt-metalized tetrakis(4-carboxyphenyl) porphyrin; nanoCoTPyP, nanocobalt 5,10,15,20-tetra(4-pyridyl)-21H,23H porphine; Mas, mycolic acids; GQDs, graphene quantum dots; FRET, fluorescence resonance energy transfer; TCPP, Tetrakis(4-carboxyphenyl)porphyrin; IP-10, IFN-γ-induced protein 10.

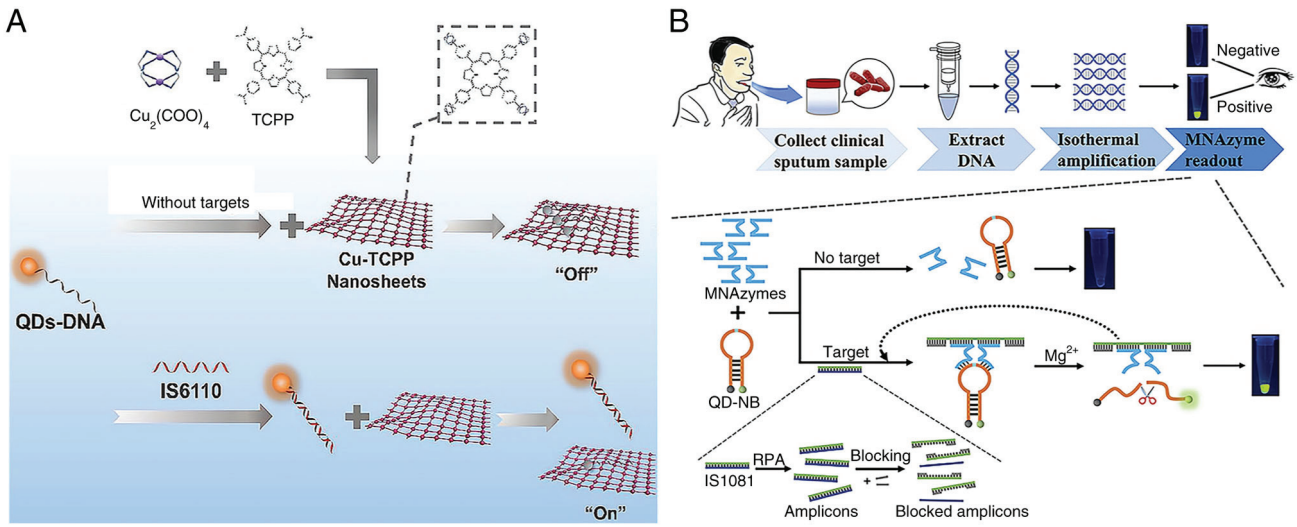

Figure 5. QD-based FRET system and colorimetric platform for TB diagnosis. (A) Schematic illustration of FRET-based MTB detection using QDs-DNA(fluorescence donor) and Cu-TCPP (fluorescence acceptor). Reproduced from (67), Copyright (2021), with permission from Elsevier. (B) Graphical representation of the QD-NB-based colorimetric platform for TB diagnosis. Reproduced from (61), Copyright (2023), with permission from American Chemical Society. FRET, fluorescence resonance energy transfer; MTB, Mycobacterium tuberculosis; QD, quantum dot; NB, nanobeacon; TB, tuberculosis.

nicotine. The platform effectively detects methyl nicotinate with a relative standard deviation <3.33%, the detection time was only 4 min and it was linear in the range of 1-100 μM with a detection limit of 0.59 μM.

With single excitation and multiple emission, QDs could identify numerous MTB markers simultaneously. This multiplexing capacity simplifies the instrumentation and experimental setup and comprehensively explains the infection's presence and severity (73,74). Zhou *et al* (20) developed an immunosensor to measure latent tuberculosis infection biomarkers (IFN-γ, TNF-α and IL-2) by embedding carbon and CdS QDs on AuNPs and magnetic beads. Then three antibody1-labeled markers were immobilized at three electrode positions to capture the corresponding antigens and simultaneously detected with antibody2 and QD functionalized nanoprobes. Hu *et al* (63) developed a novel

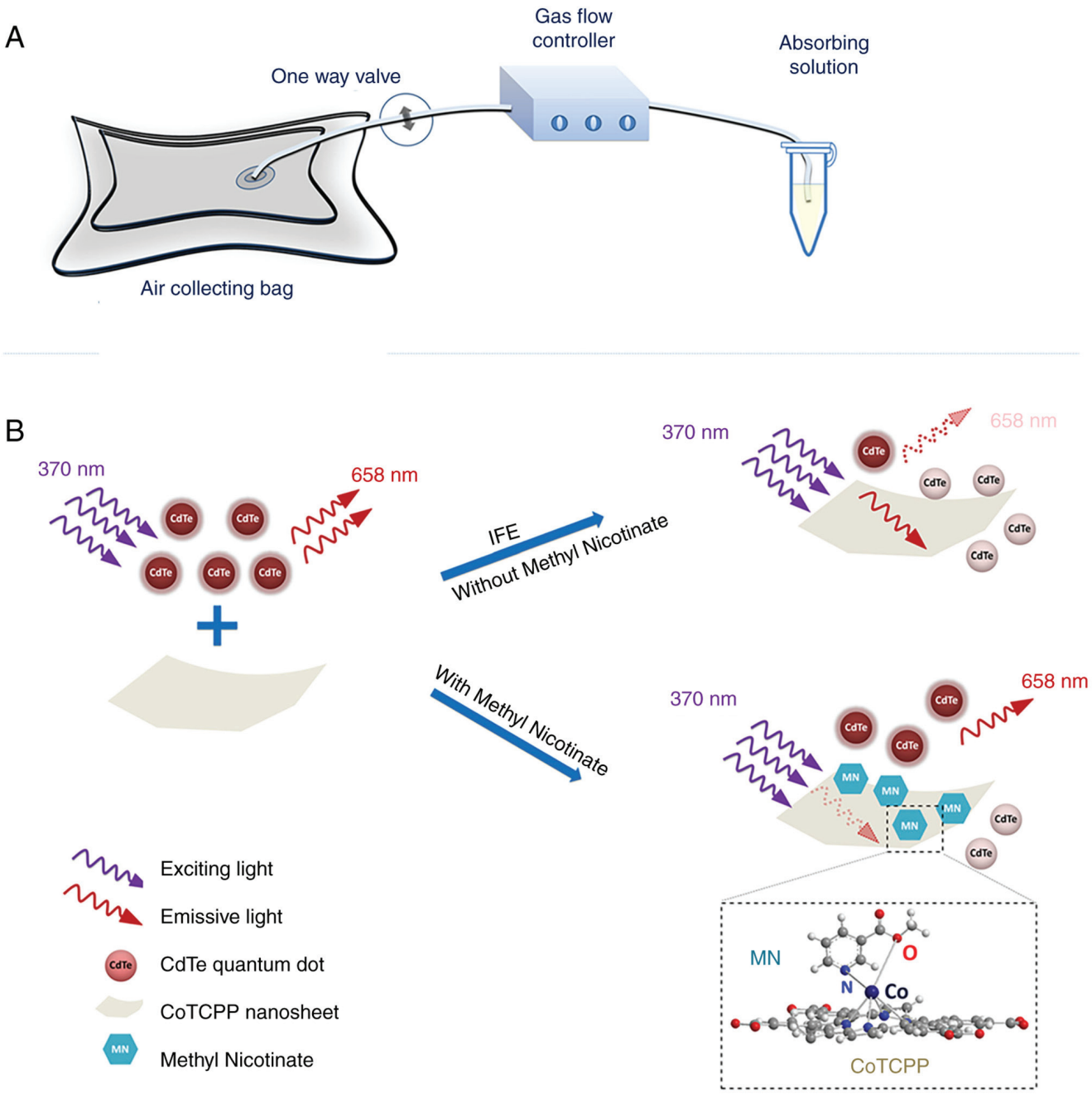

Figure 6. QDs as fluorescent signal switches to detect MTB. Schematic for (A) vapor sample collection and (B) MTB methyl nicotinate detection based on CoTCPP nanosheets CdTe QDs and CoTCPP. Reproduced from (62), Copyright (2022), with permission from Springer. MTB, Mycobacterium tuberculosis; QD, quantum dot.

fluorescence biosensor that uses nanocobalt 5,10,15,20-tetra (4-pyridyl)-21H,23H porphine (nanoCoTPyP) and dual QDs to simultaneously detect two drug-resistant genes of MTB, specifically rpoB531 and katG315 (Fig. 7). The green and red QDs were linked to the single strand (ss)DNA probes ssDNA1 and ssDNA2 and combined to form QD-ssDNA probes. These probes interact with nanoCoTPyP through electrostatic forces, π-π stacking and hydrogen bonding, resulting in fluorescence quenching through FRET and photoinduced electron transfer. This biosensor enables the concurrent quantification of the two genes in one test using the distinct emission wavelengths of the dual QDs. Notably, this approach allows for the simultaneous identification of two mutations in the PCR products of multi-drug resistant tuberculosis within a 95-min timeframe.

4. Carbon-based nanomaterials for TB diagnosis

Carbon-based nanomaterials, such as fullerene, carbon nanotubes, nanodiamonds and graphene, show great potential for TB diagnosis (75,76). These materials can be engineered to detect specific TB biomarkers, even at very low concentrations (77). Recent advances in the use of carbon-based nanomaterials for TB diagnostics are summarized in Table III. Additionally, carbon nanomaterial-based point-of-care testing devices can be portable and easily used, which is beneficial

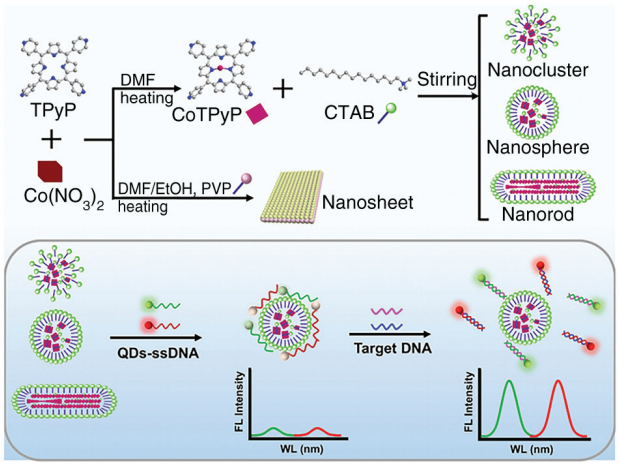

Figure 7. Schematic Illustration for preparing nanoCoTPyPs with different morphology and the simultaneous detection of rpoB531 and katG315 based on double QDs-ssDNA and nanoCoTPyP. The spherical nano-CoTPyP performed the best quenching and sensing properties. Reproduced from (63), Copyright (2022), with permission from American Chemical Society. nano-CoTPyP, nanocobalt 5,10,15,20-tetra(4-pyridyl)-21H,23H porphine; QD, quantum dot; ssDNA, single-stranded probe DNA.

in low-resource TB-endemic areas. making them particularly advantageous in low-resource, TB-endemic regions.

Graphene-based TB detection. Graphene is often employed in sensors designed as reduced graphene oxide (rGO), a cost-effective form produced via chemical and hydrothermal reduction of graphene oxide (83). rGO is favored in biosensor design for its high current density, exceptional electrocatalytic properties, extensive surface area, excellent thermal conductivity and numerous electroactive sites (90,91). However, due to van der Waals forces and its inherent laminar structure, rGO tends to aggregate, leading to a decrease in surface area and thus reducing its sensing ability (92,93). The commonly used reducing agents for rGO, such as hydrazine and $NaBH_4$, are highly toxic and hazardous (94). Chaturvedi *et al* (95) addressed this issue by reducing GO to rGO and coating it with a biocompatible, nanometer-thick polydopamine (PDA) layer. PDA is rich in functional groups such as amines, imines and catechols, facilitating dense covalent attachment of biomolecules and providing binding sites for metal nanoparticles. Consequently, they engineered a nanocomposite of rGO, PDA and AuNPs and applied it to carbon electrodes to enhance the electroactive surface area and electron transport. Electrochemical analysis using cyclic voltammetry and linear sweep voltammetry revealed a sensitivity of $2.12x10^{-3}$ mA μM^{-1} and a response time of 5 sec for target DNA detection at $0.1x10^{-7}$ mM.

PDA thin coatings improve the antifouling properties and cytocompatibility of carbon nanomaterials (96). The adhesive properties of PDA facilitate the attachment of biomolecules to biosensor transducers through physical interactions (97). Polynorepinephrine (PNE), a compound closely related to PDA, possesses additional -OH groups and superior coating uniformity; however, it has rarely been investigated in TB biosensors. (98,99). Bisht *et al* (81) researched PNE as a coating for rGO and AuNPs in the development of an electrochemical nanobiosensor targeting MTB (Fig. 8). The active rGO, coupled with the reactive quinone groups and AuNPs, synergistically forms a high-performance biosensing platform that facilitates substantial biomolecule loading and delivers an exceptional electrochemical response. The study demonstrated that the PNE-modified system (rGO/PNE/Au) outperforms the PDA-modified counterpart (rGO/PDA/Au) for the development of electrochemical biosensors. The PNE-modified system achieves a markedly higher electrochemical response and offers a surface richer in functional groups, enhancing the loading capacity for biomolecules such as probe DNA. The biosensor demonstrated high sensitivity ($2.3x10^{-3}$ mA μM^{-1}), a low detection limit ($0.1x10^{-7}$ μM) and a quick response time of 5 sec.

Paper-based analytical devices (PADs) require minimal training and are highly portable, which is crucial for field testing and point-of-care TB diagnostics (100). Graphene nanomaterials have a large surface area, which provides more active sites for biomolecule adsorption, enhancing the electrochemical properties of sensors (101). They boost the sensitivity and specificity of PADs, allowing for the detection of TB biomarkers at low concentrations. Pornprom *et al* (78) introduced a PAD biosensor using AuNP-decorated carboxyl graphene (GCOOH) to detect heat shock protein (Hsp16.3), a key TB infection biomarker. The AuNPs enhance the electrochemical properties of the sensor, while the GCOOH, with its numerous binding sites, facilitates direct antibody immobilization through carboxyl groups and primary amines. The PAD sensor specifically recognizes Hsp16.3, requiring only 5 μl sample volume, performed effectively with a detection limit of 0.01 ng/ml and quickly detected TB-infected clinical samples within 20 min.

Unlike other electrochemical sensors, field-effect transistor (FET) biosensors involve semiconductor manufacturing (102). This enables the large-scale production of these sensors, making them ideal for widespread use in assessing infection status, which is the purpose of point-of-care testing (103). Graphene-based field-effect transistors (GFETs) have a low on/off ratio compared with other semiconductor materials because they lack a bandgap. However, the low noise characteristic of GFETs can compensate for this limitation, enhancing their overall performance (104,105). Seo *et al* (82) designed a GFET biosensor for MTB MPT64 protein detection to construct an effective point-of-care TB testing platform. To efficiently conjugate antibodies, the graphene channels of the GFET were functionalized by immobilizing 1,5-diaminonaphthalene (1,5-DAN) and glutaraldehyde linker molecules. Atomic force microscopy was used to investigate the surface roughness of graphene after functionalization with MPT64 Ab and 1,5-DAN. As shown in Fig. 9, Raman spectroscopy and X-ray photoelectron spectroscopy validated the successful and uniform immobilization of linker molecules on the graphene surface and the subsequent antibody conjugation. The MPT64 antibody-functionalized GFET achieved a detection limit of 1 fg/ml in real-time and demonstrated greater sensitivity and faster detection compared with ELISA.

Single-walled carbon nanotubes-based TB detection. Single-walled carbon nanotubes (SWCNTs), another popular carbon nanomaterial, are similar in size to biomolecules and

Table III. Recent advances in carbon-based nanomaterials diagnostics for tuberculosis.

First author/s, year	Nanomaterials	Detection assays	Target	LOD	Detection Time	(Refs.)
Pornprom *et al*, 2024	AuNPs/GCOOH	Paper-based electrochemical biosensor	Hsp16.3	0.01 ng/ml	20 min	(78)
Wang *et al*, 2024	SWCNT	FET	MTB-Ag85B	0.05 fg/ml	10 min	(79)
Le *et al*, 2024	FNDs	SELFIA	ESAT6	0.02 ng/ml	NA	(80)
Bisht *et al*, 2023	RGO/PNE/Au	Electrochemical sensor	MTB DNA	10^{-8} μM	5 sec	(81)
Seo *et al*, 2023	Graphene	GFET	MPT64	1 fg/ml	NA	(82)
Mogha *et al*, 2018	rGO-PDA-Au NP	Electrochemical genosensor	MTB DNA	10^{-15} M	5 sec	(83)
Li *et al*, 2022	AQCA/CMK-3-Ce-MOFs	Electrochemical aptasensor	MPT64	67.6 fg/ml	NA	(84)
Rizi *et al*, 2021	HAPNPTs// MWCNTs	Electrochemical DNA biosensor	Genome of MTB H37Rv	0.141 nM	NA	(85)
Javed *et al*, 2021	GO-CHI	Electrochemical genosensor	IS6110	3.4 pM	NA	(86)
Omar *et al*, 2021	Ni-rGO-PANI	CV-based immunosensor	ESAT-6	1.0 ng/ml	15 min	(87)
Jaroenram *et al*, 2020	Graphene	Electrochemical genosensor	IS6110	1 pg DNA	65 min	(88)
Kahng *et al*, 2020	SWCNT	Immuno-resistive sensor	MTB/MPT64	10 CFU/ml/100 ng/ml	30 min	(89)

LOD, limit of detection; GCOOH, carboxyl graphene; Hsp, heat shock protein; SWCNTs, single-walled carbon nanotubes; FET, field-effect transistor; MTB, Mycobacterium tuberculosis; Ag85B, antigen 85B, FNDs, fluorescent nanodiamonds; SELFIA, spin-enhanced lateral flow immunoassay; ESAT-6, early secreted antigenic target-6; NA, not available; PNE, polynorepinephrine; rGO, reduced graphene oxide; GFETs, graphene-based field-effect transistors; MPT64, MTB 64 protein; PDA, polydopamine; NPs, nanoparticles; MPT64, MTB 64 protein; AQCA, anthraquinone-2-carboxylic acid; CMK-3,carbon framework; MWCNTs, multi-wall carbon nanotubes; GO-CHI, graphene oxide-chitosan.

have an average diameter of 1 nm (106). They possess low charge-carrier density and high intrinsic carrier mobility, making them ideal for detecting electrostatic interactions and charge transfer during biological processes (107). Since 1998, SWCNTs have been used to fabricate FETs, demonstrating exceptional performance in biosensing due to their distinctive physical characteristics (108). SWCNTs have advantages over graphene, silicon nitride and silicon nanowires as FET functional nanomaterials. Their tiny diameter helps reduce gate leakage and exhibit high conductivity, biocompatibility, charge mobility and stability (109,110). Researchers have constructed SWCNT-based FET biosensors to detect SARS antigens (111), cancer exosomal miRNA (112) and Alzheimer's disease biomarkers (113). The limit of detection of these biosensors is equivalent to advanced techniques such as nucleic acid amplification tests and ELISA.

Wang *et al* (79) developed a SWCNT-based FET device that was functionalized with an anti-MTB antigen 85B antibody (Ab85B) to detect the MTB-secreted antigen 85B (Ag85B). 1-ethyl-3-(3-dimethylaminopropyl)carbodiimide (EDC)/Sulfo-N-hydroxysuccinimide (NHS) coupling linked Ab85B to commercial SWCNT sidewalls via carboxyl groups (Fig. 10A). The Ab85B-SWCNT FET device successfully detected Ag85B in phosphate-buffered saline with a detection limit of 0.05 fg/ml. Furthermore, it effectively identified Ag85B spiked in artificial sputum. Additionally, bovine serum albumin-blocked Ab85B SWCNT FET devices could detect Ag85B in serum, distinguishing TB-positive clinical samples from negative ones within 10 min using a portable Metrohm potentiostat. These results demonstrate the potential practicality of the biosensor for TB diagnosis (79).

Fluorescent nanodiamonds (FNDs)-based TB detection. FNDs are carbon nanoparticles with nitrogen vacancy defects (114). The ground-state electron spins at the center of these nitrogen vacancies can be optically polarized, resulting in spin-state mixing induced by a time-varying magnetic field (115). Diagnostics of ultrasensitive sub-half-molar disease markers are possible with microwave-modulated spin resonance (116). Le *et al* (80) developed a spin-enhanced lateral flow immunoassay for TB diagnostics by conjugating FNDs with ESAT6 antibodies (Fig. 10B). This immunosensor demonstrated 100-fold higher sensitivity than traditional AuNPs-based lateral flow immunoassays. The FNDs used in this study were ~100 nm and contained ~10 ppm nitrogen-vacancy centers. By employing a lateral flow membrane strip with a pre-structured

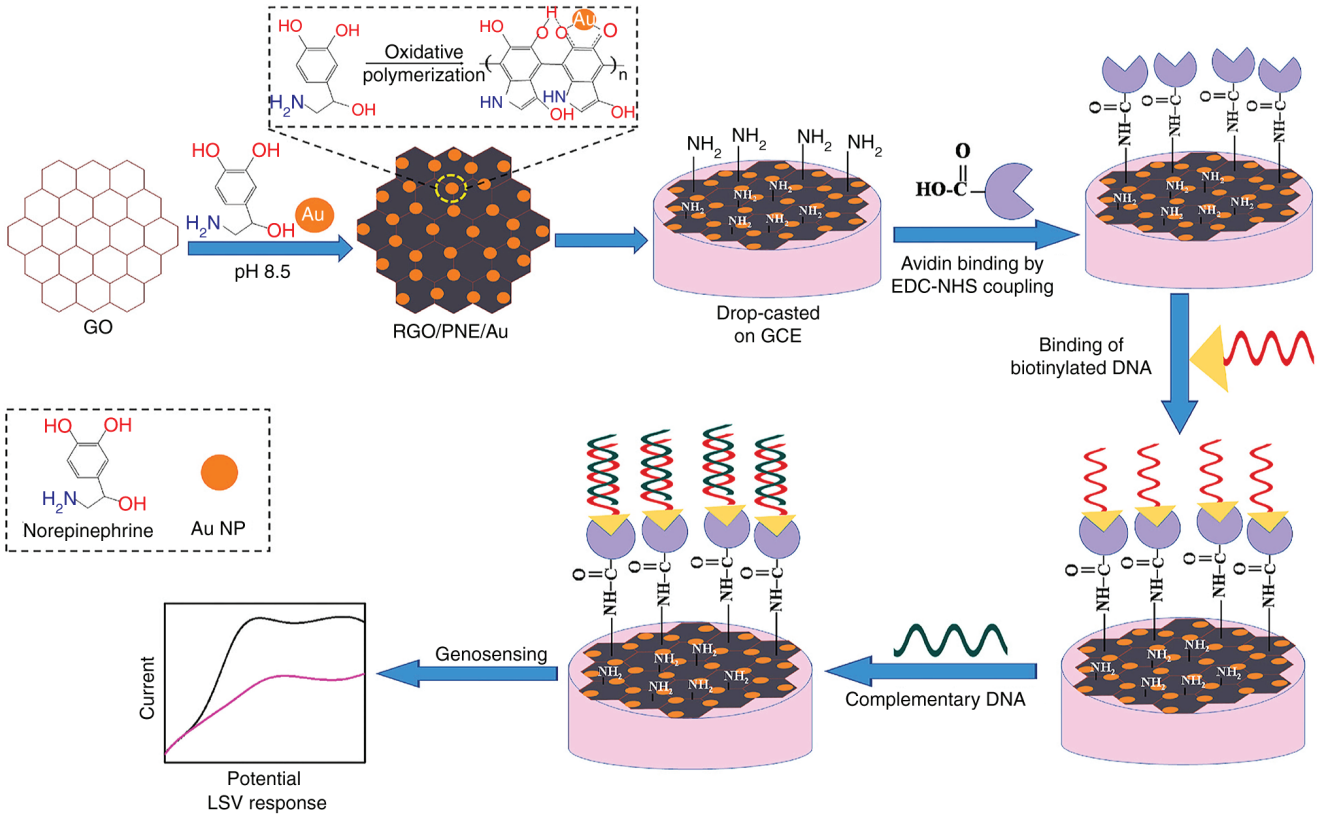

Figure 8. Schematic diagram of rGO/PNE/Au nanocomposites synthesis and detection procedure for MTB DNA. Reproduced from (81), Copyright (2022), with permission from Elsevier. rGO/PNE MTB, Mycobacterium tuberculosis; rGO, reduced graphene oxide; PNE, polynorepinephrine.

1-mm narrow channel, the detection limit for ESAT6 antigen was ~0.02 ng/ml. This FND-based magneto-optical sensor identified MTB complexes in clinical samples and distinguished TB from NTM. Moreover, the immunosensor is a simple portable device that can be used in point of care and clinics.

5. Comparison of nanomaterials for TB diagnostics

It is essential to compare the manipulation, production, stability and adaptation of these materials when selecting them for TB biosensing applications.

Ease of manipulation. AuNPs and AgNPs are user-friendly due to simple conjugation processes (117). By contrast, QDs need complex surface modifications, while MNPs and carbon nanomaterials require sophisticated handling for optimal performance (118,119).

Synthesis. AuNPs and AgNPs are straightforward to synthesize via chemical reduction (120). QD synthesis is more complex, focusing on size and shape control for optical properties (121). MNP synthesis varies by composition and size and graphene involves scalable but costly methods such as chemical vapor deposition (122).

Stability. AuNPs are stable for long-term use, while AgNPs are more susceptible to oxidation (123). QDs are photostable and MNPs remain stable in different conditions. Graphene and SWCNTs are stable but prone to aggregation, needing functionalization for improved dispersion (124).

Adaptability. AuNPs and AgNPs easily integrate into biosensors. QDs, despite toxicity concerns, offer tunable fluorescence in biosensing. MNPs are ideal for magnetic separation in assays (125). Carbon nanomaterials are adaptable for electronic and electrochemical biosensors but may require miniaturization for point-of-care use (126).

In summary, the choice of nanomaterial for TB diagnostics is application-specific, balancing manipulation ease, synthesis complexity, stability and adaptability to achieve sensitive, specific and cost-effective biosensors.

6. Limitations of nanomaterial-based sensing systems and possible solutions

While nanomaterial-based sensing systems have shown significant advances in the detection of MTB, several limitations and challenges must be addressed to fully realize their potential in TB diagnostics.

Stability and long-term performance. Nanomaterials can degrade over time, leading to reduced sensitivity and reliability of the biosensors. Factors such as environmental conditions, storage methods and interaction with biological fluids can affect their stability. Surface modification techniques, such as coating with stabilizing agents such as polyethylene glycol or thiol groups, can enhance the stability of nanomaterials.

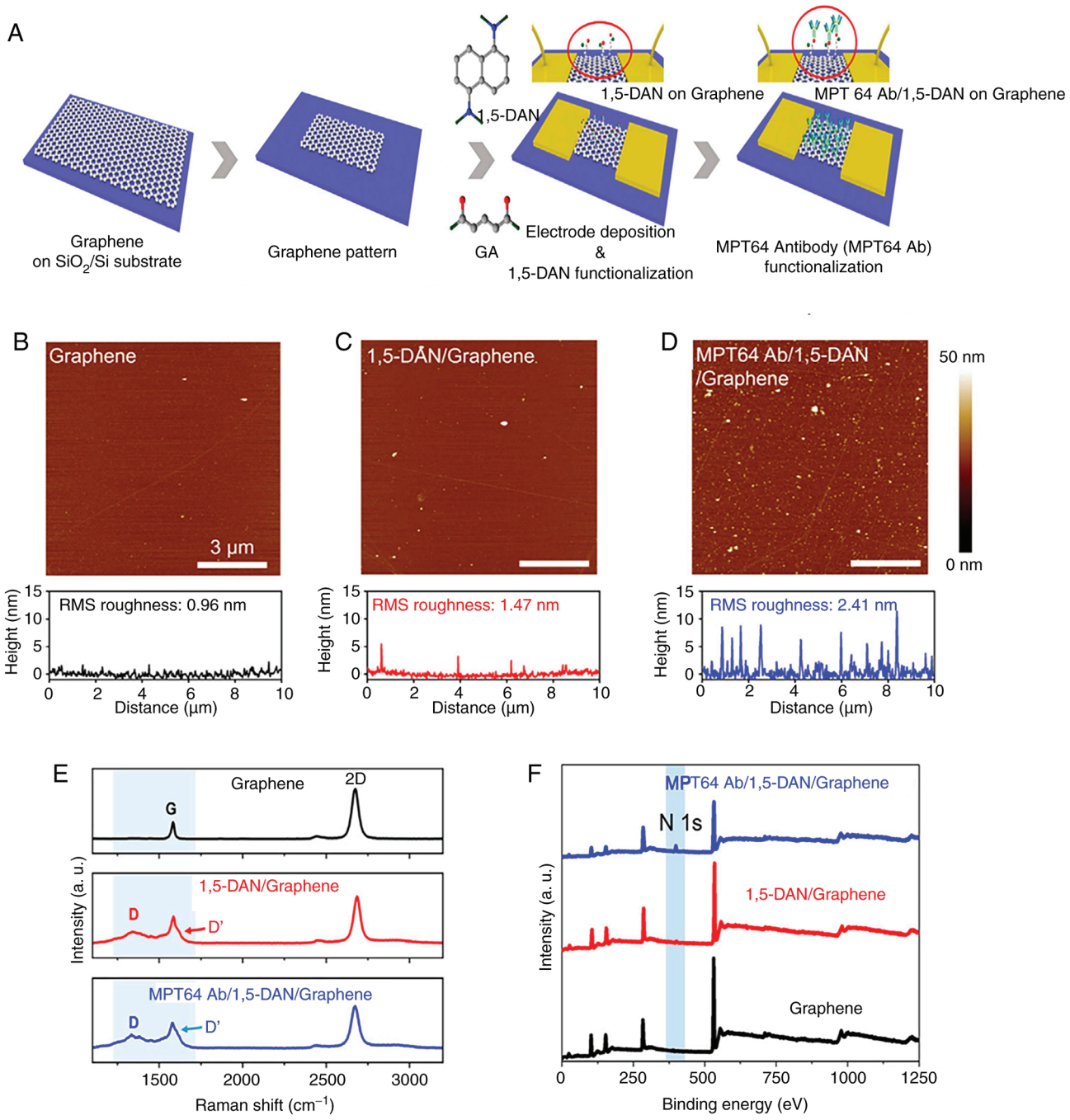

Figure 9. Graphene functionalization for the TB biosensor. (A) Illustration of surface modification of graphene-based biosensor and the coupling process of MPT64 with 1,5-DAN and glutaraldehyde. AFM photos of graphene (B) before surface modification, (C) following 1,5-DAN treatment and (D) following MTP64 Ab conjugation. (E) Raman spectroscopy and (F) X-ray photoelectron spectroscopy characterized the surface of graphene. Reproduced with permission through Creative Commons Attribution License (CC BY) from Seo G *et al* (82), Frontiers in Bioengineering and Biotechnology; published by Frontiers, 2023. TB, tuberculosis; MPT64, MTB 64 protein; 1,5-DAN, 1,5-diaminonaphthalene.

Additionally, rigorous quality control measures during manufacturing and storage can help maintain the integrity of the nanomaterials (127).

Biocompatibility and toxicity. Some nanomaterials, particularly MNPs and QDs, can exhibit toxicity when introduced into biological systems. This can lead to adverse effects on cells and tissues, limiting their use in *in vivo* diagnostics. Surface functionalization with biocompatible polymers or targeting ligands can reduce toxicity and improve cell uptake. Furthermore, developing biodegradable nanomaterials can mitigate long-term health risks (128).

Interference from biological and chemical components. Biological and chemical components in patient samples can interfere with the detection process, leading to false positives or negatives. Common interferents include proteins, lipids and other biomolecules Advanced sample preparation techniques, such as pre-concentration and purification, can reduce interference. Additionally, designing nanomaterials with specific

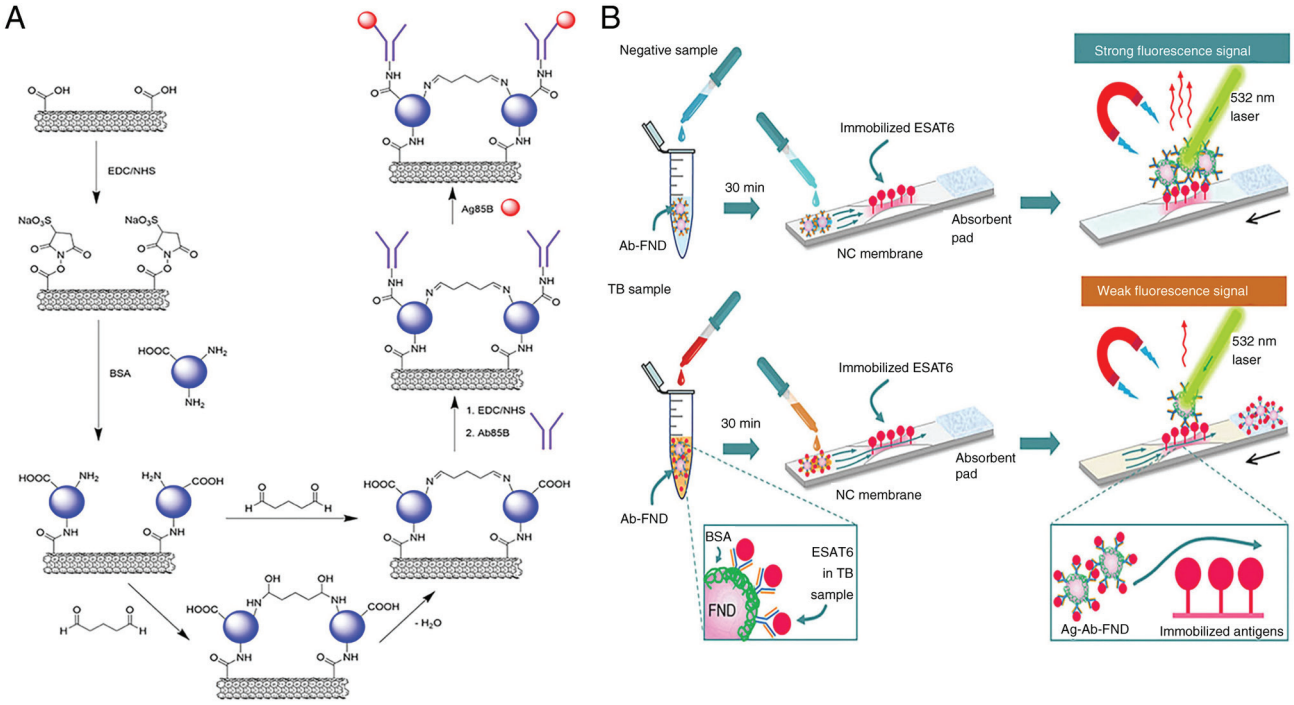

Figure 10. SWCNT-based FET device and FND-based immunosensor for MTB detection. (A) Schematic representation of SWCNTs modified by EDC/NHS and connected to Ab85B. Reproduced with permission through Creative Commons Attribution 4.0 International License from Wang J *et al* (79), ACS Sensors; published by American Chemical Society, 2024. (B) Schematic representation of ESAT6 (MTB critical virulence factor) detection by competitive spin-enhanced lateral flow immunoassay. Magnetically modulated fluorescence allows background-free detection. ESAT6 in the sample and test strip compete for the few Ab binding sites on the FND to accomplish competitive detection. Movement of the strip is indicated by a black arrow. Reproduced from (80), Copyright (2024), with permission through Creative Commons Attribution-NonCommercial 3.0 Unported Licence, Royal Society of Chemistry. SWCNTs, single-walled carbon nanotubes; EDC/NHS, 1-Ethyl-3-(3-dimethylaminopropyl)carbodiimide/N-Hydroxysuccinimide; ESAT6, early secreted antigenic target-6; FNDs, fluorescent nanodiamonds; TB, tuberculosis.

recognition elements, such as antibodies or aptamers, can enhance selectivity and reduce cross-reactivity (129).

Cost and scalability. The synthesis and functionalization of nanomaterials can be costly and technically challenging, particularly for large-scale production. High costs can limit the accessibility of these technologies in resource-limited settings. Developing cost-effective synthesis methods, such as green chemistry approaches and scalable manufacturing processes, can reduce production costs. Additionally, optimizing the use of nanomaterials to achieve the desired performance with minimal material usage can help make these technologies more affordable (24,129).

7. Comparison of different response detection technologies for TB diagnostics

In addition to the properties of nanomaterials, response detection technology plays a crucial role in the analytical performance of biosensors for TB diagnostics. Optical assays, such as those using AuNPs, offer simplicity and cost-effectiveness but may have limited sensitivity and be prone to interference from complex sample matrices (130). Fluorescence assays, often employing QDs, provide high sensitivity and specificity due to their unique optical properties, yet they require specialized equipment and can suffer from photobleaching (131). Electrochemical assays, enhanced by carbon-based nanomaterials such as graphene, are known for their high sensitivity, rapid response and low cost, but are susceptible to electrode fouling and necessitate careful handling (132). Each detection technology presents distinct advantages and challenges and the optimal choice for TB biosensors depends on the balance between sensitivity, specificity, cost and operational simplicity. The development of future biosensors should aim to integrate the strengths of these detection methods to enhance diagnostic reliability and practicality.

8. Conclusions

In conclusion, nanomaterials for MTB detection may revolutionize TB diagnostics by addressing the inadequacies of clinical approaches. Metal nanoparticles, such as gold and silver, have been employed in colorimetric and electrochemical biosensors to speed up detection. QD-based platforms, such as the QD-NB-based MNAzyme colorimetric assay and the double QDs-ssDNA probe, can detect different TB markers simultaneously and are ultra-sensitive. Carbon-based nanomaterials, such as the graphene-based PAD, can quickly detect MTB in trace specimens. In serum, SWCNT FETs rapidly distinguish TB-positive from negative samples.

Despite the promising research progress reviewed here, limitations and problems remain. For instance, biosensor stability, biocompatibility and long-term performance need improvement. New diagnostic procedures also need substantial clinical validation to assure safety, efficacy and regulatory compliance. In practice, biological and chemical components can interfere with sensors; thus, their anti-interference capabilities must be

strengthened. Researchers should improve sensor design, nanomaterial fabrication and data interpretation to overcome such challenges.

Acknowledgements

Not applicable.

Funding

No funding was received.

Availability of data and materials

Not applicable.

Authors' contributions

LC conducted the overall planning of the review, carried out the literature search and selection process. JZ drafted the core content. HW analyzed and discussed the literature in depth, offering valuable insights and assisting in refining the text. LC performed supplementary literature searches and validations, enhancing the comprehensiveness and accuracy of the review. Furthermore, JZ and LC jointly verified the authenticity of the relevant data points sourced from the reviewed literature. Data authentication is not applicable. All authors read and approved the final manuscript.

Ethics approval and consent to participate

Not applicable.

Patient consent for publication

Not applicable.

Competing interests

The authors declare that they have no competing interests.

References

1. Bagcchi S: WHO's global tuberculosis report 2022. Lancet Microbe 4: e20, 2023.
2. Asadi L, Croxen M, Heffernan C, Dhillon M, Paulsen C, Egedahl ML, Tyrrell G, Doroshenko A and Long R: How much do smear-negative patients really contribute to tuberculosis transmissions? Re-examining an old question with new tools. EClinicalMedicine 43: 101250, 2022.
3. Meriki HD, Wung NH, Tufon KA, Tony NJ, Ane-Anyangwe I and Cho-Ngwa F: Evaluation of the performance of an in-house duplex PCR assay targeting the IS6110 and rpoB genes for tuberculosis diagnosis in Cameroon. BMC Infect Dis 20: 791, 2020.
4. Natarajan S, Ranganathan M, Hanna LE and Tripathy S: Transcriptional profiling and deriving a seven-gene signature that discriminates active and latent tuberculosis: An integrative bioinformatics approach. Genes (Basel) 13: 616, 2022.
5. Molloy A, Harrison J, McGrath JS, Owen Z, Smith C, Liu X, Li X and Cox JAG: Microfluidics as a novel technique for tuberculosis: From diagnostics to drug discovery. Microorganisms 9: 2330, 2021.
6. Meier JP, Möbus S, Heigl F, Asbach-Nitzsche A, Niller HH, Plentz A, Avsar K, Heiß-Neumann M, Schaaf B, Cassens U, *et al*: Performance of T-Track® TB, a novel dual marker RT-qPCR-based whole-blood test for improved detection of active tuberculosis. Diagnostics (Basel) 13: 758, 2023.
7. Çiftci İH and Karakeçe E Comparative evaluation of TK SLC-L, a rapid liquid mycobacterial culture medium, with the MGIT system. BMC Infect Dis 14: 130, 2014.
8. Okoi C anderson STB, Antonio M, Mulwa SN, Gehre F and Adetifa IMO: Non-tuberculous mycobacteria isolated from pulmonary samples in sub-Saharan Africa-a systematic review and meta analyses. Sci Rep 7: 12002, 2017.
9. Reed JL, Walker ZJ, Basu D, Allen V, Nicol MP, Kelso DM and McFall SM: Highly sensitive sequence specific qPCR detection of Mycobacterium tuberculosis complex in respiratory specimens. Tuberculosis (Edinb) 101: 114-124, 2016.
10. Yang X, Fan S, Ma Y, Chen H, Xu JF, Pi J, Wang W and Chen G: Current progress of functional nanobiosensors for potential tuberculosis diagnosis: The novel way for TB control? Front Bioeng Biotechnol 10: 1036678, 2022.
11. Lyu M, Zhou J, Zhou Y, Chong W, Xu W, Lai H, Niu L, Hai Y, Yao X, Gong S, *et al*: From tuberculosis bedside to bench: UBE2B splicing as a potential biomarker and its regulatory mechanism. Signal Transduct Target Ther 8: 82, 2023.
12. Metcalf T, Soria J, Montano SM, Ticona E, Evans CA, Huaroto L, Kasper M, Ramos ES, Mori N, Jittamala P, *et al*: Evaluation of the GeneXpert MTB/RIF in patients with presumptive tuberculous meningitis. PLoS One 13: e0198695, 2018.
13. Tu Phan LM, Tufa LT, Kim HJ, Lee J and Park TJ: Trends in diagnosis for active tuberculosis using nanomaterials. Curr Med Chem 26: 1946-1959, 2019.
14. Joshi H, Kandari D, Maitra SS and Bhatnagar R: Biosensors for the detection of Mycobacterium tuberculosis: A comprehensive overview. Crit Rev Microbiol 48: 784-812, 2022.
15. Pourakbari R, Shadjou N, Yousefi H, Isildak I, Yousefi M, Rashidi MR and Khalilzadeh B: Recent progress in nanomaterial-based electrochemical biosensors for pathogenic bacteria. Mikrochim Acta 186: 820, 2019.
16. Uhuo OV, Waryo TT, Douman SF, Januarie KC, Nwambaekwe KC, Ndipingwi MM, Ekwere P and Iwuoha EI: Bioanalytical methods encompassing label-free and labeled tuberculosis aptasensors: A review. Anal Chim Acta 1234: 340326, 2022.
17. Xu K, Liang ZC, Ding X, Hu H, Liu S, Nurmik M, Bi S, Hu F, Ji Z, Ren J, *et al*: Nanomaterials in the prevention, diagnosis, and treatment of Mycobacterium tuberculosis infections. Adv Healthc Mater 7: 1700509, 2018.
18. Tan P, Li H, Wang J and Gopinath SCB: Silver nanoparticle in biosensor and bioimaging: Clinical perspectives. Biotechnol Appl Biochem 68: 1236-1242, 2021.
19. Muthukrishnan L: Multidrug resistant tuberculosis-diagnostic challenges and its conquering by nanotechnology approach-an overview. Chem Biol Interact 337: 109397, 2021.
20. Zhou B, Zhu M, Hao Y and Yang P: Potential-resolved electrochemiluminescence for simultaneous determination of triple latent tuberculosis infection markers. ACS Appl Mater Interfaces 9: 30536-30542, 2017.
21. Dykman L and Khlebtsov N: Gold nanoparticles in biomedical applications: Recent advances and perspectives. Chem Soc Rev 41: 2256-2282, 2012.
22. Sapsford KE, Algar WR, Berti L, Gemmill KB, Casey BJ, Oh E, Stewart MH and Medintz IL: Functionalizing nanoparticles with biological molecules: Developing chemistries that facilitate nanotechnology. Chem Rev 113: 1904-2074, 2013.
23. Drain PK, Bajema KL, Dowdy D, Dheda K, Naidoo K, Schumacher SG, Ma S, Meermeier E, Lewinsohn DM and Sherman DR: Incipient and subclinical tuberculosis: A clinical review of early stages and progression of infection. Clin Microbiol Rev 31: e00021-18, 2018.
24. Rosi NL and Mirkin CA: Nanostructures in biodiagnostics. Chem Rev 105: 1547-1562, 2005.
25. Singh V and Chibale K: Strategies to combat multi-drug resistance in tuberculosis. Acc Chem Res 54: 2361-2376, 2021.
26. Golichenari B, Nosrati R, Farokhi-Fard A, Abnous K, Vaziri F and Behravan J: Nano-biosensing approaches on tuberculosis: Defy of aptamers. Biosens Bioelectron 117: 319-331, 2018.
27. Eivazzadeh-Keihan R, Saadatidizaji Z, Mahdavi M, Maleki A, Irani M and Zare I: Recent advances in gold nanoparticles-based biosensors for tuberculosis determination. Talanta 275: 126099, 2024.
28. Golichenari B, Nosrati R, Farokhi-Fard A, Faal Maleki M, Gheibi Hayat SM, Ghazvini K, Vaziri F and Behravan J: Electrochemical-based biosensors for detection of Mycobacterium tuberculosis and tuberculosis biomarkers. Crit Rev Biotechnol 39: 1056-1077, 2019.

29. Seele PP, Dyan B, Skepu A, Maserumule C and Sibuyi NRS: Development of gold-nanoparticle-based lateral flow immunoassays for rapid detection of TB ESAT-6 and CFP-10. Biosensors (Basel) 13: 354, 2023.
30. Kamra E, Prasad T, Rais A, Dahiya B, Sheoran A, Soni A, Sharma S and Mehta PK: Diagnosis of genitourinary tuberculosis: Detection of mycobacterial lipoarabinomannan and MPT-64 biomarkers within urine extracellular vesicles by nano-based immuno-PCR assay. Sci Rep 13: 11560, 2023.
31. Dahiya B, Prasad T, Rais A, Sheoran A, Kamra E, Mor P, Soni A, Sharma S and Mehta PK: Quantification of mycobacterial proteins in extrapulmonary tuberculosis cases by nano-based real-time immuno-PCR. Future Microbiol 18: 771-783, 2023.
32. Tripathi A, Jain R and Dandekar P: Rapid visual detection of Mycobacterium tuberculosis DNA using gold nanoparticles. Anal Methods 15: 2497-2504, 2023.
33. Huang H, Chen Y, Zuo J, Deng C, Fan J, Bai L and Guo S: MXene-incorporated C^{60}NPs and Au@Pt with dual-electric signal outputs for accurate detection of Mycobacterium tuberculosis ESAT-6 antigen. Biosens Bioelectron 242: 115734, 2023.
34. Patnaik N and Dey RJ: Label-free citrate-stabilized silver nanoparticles-based, highly sensitive, cost-effective, and rapid visual method for the differential detection of Mycobacterium tuberculosis and mycobacterium bovis. ACS Infect Dis 10: 426-435, 2024.
35. Pei X, Hong H, Liu S and Li N: Nucleic acids detection for Mycobacterium tuberculosis based on gold nanoparticles counting and rolling-circle amplification. Biosensors (Basel) 12: 448, 2022.
36. León-Janampa N, Shinkaruk S, Gilman RH, Kirwan DE, Fouquet E, Szlosek M, Sheen P and Zimic M: Biorecognition and detection of antigens from Mycobacterium tuberculosis using a sandwich ELISA associated with magnetic nanoparticles. J Pharm Biomed Anal 215: 114749, 2022.
37. Zhang J and He F: Mycobacterium tuberculosis piezoelectric sensor based on AuNPs-mediated enzyme assisted signal amplification. Talanta 236: 122902, 2022.
38. Xie J, Mu Z, Yan B, Wang J, Zhou J and Bai L: An electrochemical aptasensor for Mycobacterium tuberculosis ESAT-6 antigen detection using bimetallic organic framework. Mikrochim Acta 188: 404, 2021.
39. Prabowo BA, Purwidyantri A, Liu B, Lai HC and Liu KC: Gold nanoparticle-assisted plasmonic enhancement for DNA detection on a graphene-based portable surface plasmon resonance sensor. Nanotechnology 32: 095503, 2021.
40. Tai MJY, Perumal V, Gopinath SCB, Raja PB, Ibrahim MNM, Jantan IN, Suhaimi NSH and Liu WW: Laser-scribed graphene nanofiber decorated with oil palm lignin capped silver nanoparticles: A green biosensor. Sci Rep 11: 5475, 2021.
41. Mohd Azmi UZ, Yusof NA, Abdullah J, Alang Ahmad SA, Mohd Faudzi FN, Ahmad Raston NH, Suraiya S, Ong PS, Krishnan D and Sahar NK: Portable electrochemical immunosensor for detection of Mycobacterium tuberculosis secreted protein CFP10-ESAT6 in clinical sputum samples. Mikrochim Acta 188: 20, 2021.
42. Gupta S, Bhatter P and Kakkar V: Point-of-care detection of tuberculosis using magnetoresistive biosensing chip. Tuberculosis (Edinb) 127: 102055, 2021.
43. León-Janampa N, Zimic M, Shinkaruk S, Quispe-Marcatoma J, Gutarra A, Le Bourdon G, Gayot M, Changanaqui K, Gilman RH, Fouquet E, *et al*: Synthesis, characterization and bio-functionalization of magnetic nanoparticles to improve the diagnosis of tuberculosis. Nanotechnology 31: 175101, 2020.
44. Terefinko D, Dzimitrowicz A, Bielawska-Pohl A, Klimczak A, Pohl P and Jamroz P: The influence of cold atmospheric pressure plasma-treated media on the cell viability, motility, and induction of apoptosis in in human non-metastatic (MCF7) and metastatic (MDA-MB-231) breast cancer cell lines. Int J Mol Sci 22: 3855, 2021.
45. Gupta AK, Singh A and Singh S: Diagnosis of Tuberculosis: Nanodiagnostics Approaches. In: Saxena S and Khurana S (eds) NanoBioMedicine. Springer, Singapore, pp261-283, 2020.
46. Cordeiro M, Ferreira Carlos F, Pedrosa P, Lopez A and Baptista PV: Gold nanoparticles for diagnostics: Advances towards points of care. Diagnostics (Basel) 6: 43, 2016.
47. Wang Y, Yu L, Kong X and Sun L: Application of nanodiagnostics in point-of-care tests for infectious diseases. Int J Nanomedicine 12: 4789-4803, 2017.
48. Chowdhury NK, Choudhury R, Gogoi B, Chang CM and Pandey RP: Microbial synthesis of gold nanoparticles and their application. Curr Drug Targets 23: 752-760, 2022.
49. Lopes TS, Alves GG, Pereira MR, Granjeiro JM and Leite PEC: Advances and potential application of gold nanoparticles in nanomedicine. J Cell Biochem 120: 16370-16378, 2019.
50. Anker JN, Hall WP, Lyandres O, Shah NC, Zhao J and Van Duyne RP: Biosensing with plasmonic nanosensors. Nat Mater 7: 442-453, 2008.
51. Datta M, Desai D and Kumar A: Gene specific DNA sensors for diagnosis of pathogenic infections. Indian J Microbiol 57: 139-147, 2017.
52. Mi X, He F, Xiang M, Lian Y and Yi S: Novel phage amplified multichannel series piezoelectric quartz crystal sensor for rapid and sensitive detection of Mycobacterium tuberculosis. Anal Chem 84: 939-946, 2012.
53. Zhang X, Feng Y, Duan S, Su L, Zhang J and He F: Mycobacterium tuberculosis strain H37Rv electrochemical sensor mediated by aptamer and AuNPs-DNA. ACS Sens 4: 849-855, 2019.
54. Teengam P, Siangproh W, Tuantranont A, Vilaivan T, Chailapakul O and Henry CS: Multiplex paper-based colorimetric DNA sensor using pyrrolidinyl peptide nucleic acid-induced AgNPs aggregation for detecting MERS-CoV, MTB, and HPV oligonucleotides. Anal Chem 89: 5428-5435, 2017.
55. Pascu B, Negrea A, Ciopec M, Duteanu N, Negrea P, Bumm LA, Grad mBuriac O, Nemeş NS, Mihalcea C and Duda-Seiman DM: Silver nanoparticle synthesis via photochemical reduction with sodium citrate. Int J Mol Sci 24: 255, 2022.
56. Iravani S, Korbekandi H, Mirmohammadi SV and Zolfaghari B: Synthesis of silver nanoparticles: Chemical, physical and biological methods. Res Pharm Sci 9: 385-406, 2014.
57. Salvador M, Marqués-Fernandez JL, Martinez-Garcia JC, Fiorani D, Arosio P, Avolio M, Brero F, Balanean F, Guerrini A, Sangregorio C, *et al*: Double-layer fatty acid nanoparticles as a multiplatform for diagnostics and therapy. Nanomaterials (Basel) 12: 205, 2022.
58. Cheon HJ, Lee SM, Kim SR, Shin HY, Seo YH, Cho YK, Lee SP and Kim MI: Colorimetric detection of MPT64 antibody based on an aptamer adsorbed magnetic nanoparticles for diagnosis of tuberculosis. J Nanosci Nanotechnol 19: 622-626, 2019.
59. Yan Z, Gan N, Zhang H, Wang D, Qiao L, Cao Y, Li T and Hu F: A sandwich-hybridization assay for simultaneous determination of HIV and tuberculosis DNA targets based on signal amplification by quantum dots-PowerVision™ polymer coding nanotracers. Biosens Bioelectron 71: 207-213, 2015.
60. Chen P, Meng Y, Liu T, Peng W, Gao Y, He Y, Qu R, Zhang C, Hu W and Ying B: Sensitive urine immunoassay for visualization of lipoarabinomannan for noninvasive tuberculosis diagnosis. ACS Nano 17: 6998-7006, 2023.
61. Hu O, Li Z, Wu J, Tan Y, Chen Z and Tong Y: A multicomponent nucleic acid enzyme-cleavable quantum dot nanobeacon for highly sensitive diagnosis of tuberculosis with the naked eye. ACS Sens 8: 254-262, 2023.
62. He Q, Cai S, Wu J, Hu O, Liang L and Chen Z: Determination of tuberculosis-related volatile organic biomarker methyl nicotinate in vapor using fluorescent assay based on quantum dots and cobalt-containing porphyrin nanosheets. Mikrochim Acta 189: 108, 2022.
63. Hu O, Li Z, He Q, Tong Y, Tan Y and Chen Z: Fluorescence biosensor for one-step simultaneous detection of Mycobacterium tuberculosis multidrug-resistant genes using nanoCoTPyP and double quantum dots. Anal Chem 94: 7918-7927, 2022.
64. Kabwe KP, Nsibande SA, Lemmer Y, Pilcher LA and Forbes PBC: Synthesis and characterisation of quantum dots coupled to mycolic acids as a water-soluble fluorescent probe for potential lateral flow detection of antibodies and diagnosis of tuberculosis. Luminescence 37: 278-289, 2022.
65. Shi T, Jiang P, Peng W, Meng Y, Ying B and Chen P: Nucleic acid and nanomaterial synergistic amplification enables dual targets of ultrasensitive fluorescence quantification to improve the efficacy of clinical tuberculosis diagnosis. ACS Appl Mater Interfaces 16: 14510-14519, 2024.
66. Kabwe KP, Nsibande SA, Pilcher LA and Forbes PBC: Development of a mycolic acid-graphene quantum dot probe as a potential tuberculosis biosensor. Luminescence 37: 1881-1890, 2022.
67. Liang L, Chen M, Tong Y, Tan W and Chen Z: Detection of Mycobacterium tuberculosis IS6110 gene fragment by fluorescent biosensor based on FRET between two-dimensional metal-organic framework and quantum dots-labeled DNA probe. Anal Chim Acta 1186: 339090, 2021.

68. Mohd Bakhori N, Yusof NA, Abdullah J, Wasoh H, Ab Rahman SK and Abd Rahman SF: Surface enhanced CdSe/ZnS QD/SiNP electrochemical immunosensor for the detection of Mycobacterium tuberculosis by combination of CFP10-ESAT6 for better diagnostic specificity. Materials (Basel) 13: 149, 2019.
69. Qian J, Cui H, Lu X, Wang C, An K, Hao N and Wang K: Bi-color FRET from two nano-donors to a single nano-acceptor: A universal aptasensing platform for simultaneous determination of dual targets. Chem Eng J 401: 126017, 2020.
70. Zhang LM, Li R, Zhao XC, Zhang Q and Luo XL: Increased transfusion of fresh frozen plasma is associated with mortality or worse functional outcomes after severe traumatic brain injury: A retrospective study. World Neurosurg 104: 381-389, 2017.
71. Zhang X, Hu Y, Yang X, Tang Y, Han S, Kang A, Deng H, Chi Y, Zhu D and Lu Y: FÖrster resonance energy transfer (FRET)-based biosensors for biological applications. Biosens Bioelectron 138: 111314, 2019.
72. Chen S, Yu YL and Wang JH: Inner filter effect-based fluorescent sensing systems: A review. Anal Chim Acta 999: 13-26, 2018.
73. Afsari HS, Cardoso Dos Santos M, Lindén S, Chen T, Qiu X, van Bergen En Henegouwen PM, Jennings TL, Susumu K, Medintz IL, Hildebrandt N and Miller LW: Time-gated FRET nanoassemblies for rapid and sensitive intra- and extracellular fluorescence imaging. Sci Adv 2: e1600265, 2016.
74. Gliddon HD, Howes PD, Kaforou M, Levin M and Stevens MM: A nucleic acid strand displacement system for the multiplexed detection of tuberculosis-specific mRNA using quantum dots. Nanoscale 8: 10087-10095, 2016.
75. Futane A, Narayanamurthy V, Jadhav P and Srinivasan A: Aptamer-based rapid diagnosis for point-of-care application. Microfluid Nanofluidics 27: 15, 2023.
76. Kumar S, Wang Z, Zhang W, Liu X, Li M, Li G, Zhang B and Singh R: Optically active nanomaterials and its biosensing applications-a review. Biosensors (Basel) 13: 85, 2023.
77. Sharifi S, Vahed SZ, Ahmadian E, Dizaj SM, Eftekhari A, Khalilov R, Ahmadi M, Hamidi-Asl E and Labib M: Detection of pathogenic bacteria via nanomaterials-modified aptasensors. Biosens Bioelectron 150: 111933, 2020.
78. Pornprom T, Phusi N, Thongdee P, Pakamwong B, Sangswan J, Kamsri P, Punkvang A, Suttisintong K, Leanpolchareanchai J, Hongmanee P, *et al*: Toward the early diagnosis of tuberculosis: A gold particle-decorated graphene-modified paper-based electrochemical biosensor for Hsp16.3 detection. Talanta 267: 125210, 2024.
79. Wang J, Shao W, Liu Z, Kesavan G, Zeng Z, Shurin MR and Star A: Diagnostics of tuberculosis with single-walled carbon nanotube-based field-effect transistors. ACS Sens 9: 1957-1966, 2024.
80. Le TN, Descanzo MJN, Hsiao WWW, Soo PC, Peng WP and Chang HC: Fluorescent nanodiamond immunosensors for clinical diagnostics of tuberculosis. J Mater Chem B 12: 3533-3542, 2024.
81. Bisht N, Patel M, Dwivedi N, Kumar P, Mondal DP, Srivastava AK and Dhand C: Bio-inspired polynorepinephrine based nanocoatings for reduced graphene oxide/gold nanoparticles composite for high-performance biosensing of Mycobacterium tuberculosis. Environ Res 227: 115684, 2023.
82. Seo G, Lee G, Kim W, An I, Choi M, Jang S, Park YJ, Lee JO, Cho D and Park EC: Ultrasensitive biosensing platform for Mycobacterium tuberculosis detection based on functionalized graphene devices. Front Bioeng Biotechnol 11: 1313494, 2023.
83. Mogha NK, Sahu V, Sharma RK and Masram DT: Reduced graphene oxide nanoribbon immobilized gold nanoparticle based electrochemical DNA biosensor for the detection of Mycobacterium tuberculosis. J Mater Chem B 6: 5181-5187, 2018.
84. Li Y, Peng D, Guo S, Yang B, Zhou J, Zhou J, Zhang Q and Bai L: Aptasensor for Mycobacterium tuberculosis antigen MPT64 detection using anthraquinone derivative confined in ordered mesoporous carbon as a new redox nanoprobe. Bioelectrochemistry 147: 108209, 2022.
85. Rizi KS, Hatamluyi B, Rezayi M, Meshkat Z, Sankian M, Ghazvini K, Farsiani H and Aryan E: Response surface methodology optimized electrochemical DNA biosensor based on HAPNPTs/PPY/MWCNTs nanocomposite for detecting Mycobacterium tuberculosis. Talanta 226: 122099, 2021.
86. Javed A, Abbas SR, Hashmi MU, Babar NUA and Hussain I: Graphene oxide based electrochemical genosensor for label free detection of mycobacterium tuberculosis from raw clinical samples. Int J Nanomedicine 16: 7339-7352, 2021.
87. Omar RA, Verma N and Arora PK: Development of ESAT-6 based immunosensor for the detection of mycobacterium tuberculosis. Front Immunol 12: 653853, 2021.
88. Jaroenram W, Kampeera J, Arunrut N, Karuwan C, Sappat A, Khumwan P, Jaitrong S, Boonnak K, Prammananan T, Chaiprasert A, *et al*: Graphene-based electrochemical genosensor incorporated loop-mediated isothermal amplification for rapid on-site detection of Mycobacterium tuberculosis. J Pharm Biomed Anal 186: 113333, 2020.
89. Kahng SJ, Soelberg SD, Fondjo F, Kim JH, Furlong CE and Chung JH: Carbon nanotube-based thin-film resistive sensor for point-of-care screening of tuberculosis. Biomed Microdevices 22: 50, 2020.
90. Hidayah NMS, Liu WW, Lai CW, Noriman NZ, Khe CS, Hashim U and Lee HC: Comparison on graphite, graphene oxide and reduced graphene oxide: Synthesis and characterization. AIP Conf Proc 1892: 150002, 2017.
91. Ping J, Zhou Y, Wu Y, Papper V, Boujday S, Marks RS and Steele TW: Recent advances in aptasensors based on graphene and graphene-like nanomaterials. Biosens Bioelectron 64: 373-385, 2015.
92. Raccichini R, Varzi A, Passerini S and Scrosati B: The role of graphene for electrochemical energy storage. Nat Mater 14: 271-279, 2015.
93. Yan Q, Zhi N, Yang L, Xu G, Feng Q, Zhang Q and Sun S: A highly sensitive uric acid electrochemical biosensor based on a nano-cube cuprous oxide/ferrocene/uricase modified glassy carbon electrode. Sci Rep 10: 10607, 2020.
94. Barra A, Nunes C, Ruiz-Hitzky E and Ferreira P: Green carbon nanostructures for functional composite materials. Int J Mol Sci 23: 1848, 2022.
95. Chaturvedi M, Patel M, Bisht N, Shruti, Das Mukherjee M, Tiwari A, Mondal DP, Srivastava AK, Dwivedi N and Dhand C: Reduced graphene oxide-polydopamine-gold nanoparticles: A ternary nanocomposite-based electrochemical genosensor for rapid and early Mycobacterium tuberculosis detection. Biosensors (Basel) 13: 342, 2023.
96. Tian J, Deng SY, Li DL, Shan D, He W, Zhang XJ and Shi Y: Bioinspired polydopamine as the scaffold for the active AuNPs anchoring and the chemical simultaneously reduced graphene oxide: Characterization and the enhanced biosensing application. Biosens Bioelectron 49: 466-471, 2013.
97. Li Y, Shi S, Cao H, Zhao Z, Su C and Wen H: Improvement of the antifouling performance and stability of an anion exchange membrane by surface modification with graphene oxide (GO) and polydopamine (PDA). J Memb Sci 566: 44-53, 2018.
98. Xia L, Vemuri B, Gadhamshetty V and Kilduff J: Poly (ether sulfone) membrane surface modification using norepinephrine to mitigate fouling. J Memb Sci 598: 117657, 2020.
99. Dhand C, Ong ST, Dwivedi N, Diaz SM, Venugopal JR, Navaneethan B, Fazil MH, Liu S, Seitz V, Wintermantel E, *et al*: Bio-inspired in situ crosslinking and mineralization of electrospun collagen scaffolds for bone tissue engineering. Biomaterials 104: 323-338, 2016.
100. Teengam P, Siangproh W, Tuantranont A, Vilaivan T, Chailapakul O and Henry CS: Electrochemical impedance-based DNA sensor using pyrrolidinyl peptide nucleic acids for tuberculosis detection. Anal Chim Acta 1044: 102-109, 2018.
101. Thangamuthu M, Hsieh KY, Kumar PV and Chen GY: Graphene- and graphene oxide-based nanocomposite platforms for electrochemical biosensing applications. Int J Mol Sci 20: 2975, 2019.
102. Vu CA and Chen WY: Field-effect transistor biosensors for biomedical applications: Recent advances and future prospects. Sensors (Basel) 19: 4214, 2019.
103. Chen S and Bashir R: Advances in field-effect biosensors towards point-of-use. Nanotechnology 34: 492002, 2023.
104. Szunerits S, Rodrigues T, Bagale R, Happy H, Boukherroub R and Knoll W: Graphene-based field-effect transistors for biosensing: Where is the field heading to? Anal Bioanal Chem 416: 2137-2150, 2024.
105. Krishnan SK, Nataraj N, Meyyappan M and Pal U: Graphene-based field-effect transistors in biosensing and neural interfacing applications: Recent advances and prospects. Anal Chem 95: 2590-2622, 2023.
106. Gong X, Shuai L, Beingessner RL, Yamazaki T, Shen J, Kuehne M, Jones K, Fenniri H and Strano MS: Size selective corona interactions from self-assembled rosette and single-walled carbon nanotubes. Small 18: e2104951, 2022.

107. Kumar THV, Rajendran J, Atchudan R, Arya S, Govindasamy M, Habila MA and Sundramoorthy AK: Cobalt ferrite/semiconducting single-walled carbon nanotubes based field-effect transistor for determination of carbamate pesticides. Environ Res 238: 117193, 2023.
108. Liu H, Liu F, Sun Z, Cai X, Sun H, Kai Y, Chen L and Jiang C: Single layer aligned semiconducting single-walled carbon nanotube array with high linear density. Nanotechnology 33: 375301, 2022.
109. Wang Y, Liu D, Zhang H, Wang J, Du R, Li TT, Qian J, Hu Y and Huang S: Methylation-induced reversible metallic-semiconducting transition of single-walled carbon nanotube arrays for high-performance field-effect transistors. Nano Lett 20: 496-501, 2020.
110. Tran TT, Clark K, Ma W and Mulchandani A: Detection of a secreted protein biomarker for citrus Huanglongbing using a single-walled carbon nanotubes-based chemiresistive biosensor. Biosens Bioelectron 147: 111766, 2020.
111. Shao W, Shurin MR, Wheeler SE, He X and Star A: Rapid detection of SARS-CoV-2 Antigens using high-purity semiconducting single-walled carbon nanotube-based field-effect transistors. ACS Appl Mater Interfaces 13: 10321-10327, 2021.
112. Li T, Liang Y, Li J, Yu Y, Xiao MM, Ni W, Zhang Z and Zhang GJ: Carbon nanotube field-effect transistor biosensor for ultrasensitive and label-free detection of breast cancer exosomal miRNA21. Anal Chem 93: 15501-15507, 2021.
113. Chen H, Xiao M, He J, Zhang Y, Liang Y, Liu H and Zhang Z: Aptamer-functionalized carbon nanotube field-effect transistor biosensors for Alzheimer's disease serum biomarker detection. ACS Sens 7: 2075-2083, 2022.
114. Hui YY, Chen OJ, Lin HH, Su YK, Chen KY, Wang CY, Hsiao WW and Chang HC: Magnetically modulated fluorescence of nitrogen-vacancy centers in nanodiamonds for ultrasensitive biomedical analysis. Anal Chem 93: 7140-7147, 2021.
115. Boruah A and Saikia BK: Synthesis, characterization, properties and novel applications of fluorescent nanodiamonds. J Fluoresc 32: 863-885, 2022.
116. Mzyk A, Sigaeva A and Schirhagl R: Relaxometry with nitrogen vacancy (NV) centers in diamond. Acc Chem Res 55: 3572-3580, 2022.
117. Daniel MC and Astruc D: Gold nanoparticles: Assembly, supramolecular chemistry, quantum-size-related properties, and applications toward biology, catalysis, and nanotechnology. Chem Rev 104: 293-346, 2004.
118. Medintz IL, Uyeda HT, Goldman ER and Mattoussi H: Quantum dot bioconjugates for imaging, labelling and sensing. Nat Mater 4: 435-446, 2005.
119. Wei Y and Yang R: Nanomechanics of graphene. Natl Sci Rev 6: 324-348, 2019.
120. Eckhardt S, Brunetto PS, Gagnon J, Priebe M, Giese B and Fromm KM: Nanobio silver: Its interactions with peptides and bacteria, and its uses in medicine. Chem Rev 113: 4708-4754, 2013.
121. Zhao P, Xu Q, Tao J, Jin Z, Pan Y, Yu C and Yu Z: Near infrared quantum dots in biomedical applications: Current status and future perspective. Wiley Interdiscip Rev Nanomed Nanobiotechnol 10: e1483, 2018.
122. Laurent S, Bridot JL, Elst LV and Muller RN: Magnetic iron oxide nanoparticles for biomedical applications. Future Med Chem 2: 427-449, 2010.
123. Haiss W, Thanh NT, Aveyard J and Fernig DG: Determination of size and concentration of gold nanoparticles from UV-vis spectra. Anal Chem 79: 4215-4221, 2007.
124. Kim D, Shin K, Kwon SG and Hyeon T: Synthesis and biomedical applications of multifunctional nanoparticles. Adv Mater 30: e1802309, 2018.
125. Sobhanan J, Anas A and Biju V: Nanomaterials for fluorescence and multimodal bioimaging. Chem Rec 23: e202200253, 2023.
126. Katz E and Willner I: Integrated nanoparticle-biomolecule hybrid systems: Synthesis, properties, and applications. Angew Chem Int Ed Engl 43: 6042-6108, 2004.
127. Li B, Wang W, Zhao L, Wu Y, Li X, Yan D, Gao Q, Yan Y, Zhang J, Feng Y, *et al*: Photothermal therapy of tuberculosis using targeting pre-activated macrophage membrane-coated nanoparticles. Nat Nanotechnol 19: 834-845, 2024.
128. Nair A, Greeny A, Nandan A, Sah RK, Jose A, Dyawanapelly S, Junnuthula V, K V A and Sadanandan P: Advanced drug delivery and therapeutic strategies for tuberculosis treatment. J Nanobiotechnology 21: 414, 2023.
129. El-Samadony H, Althani A, Tageldin MA and Azzazy HME: Nanodiagnostics for tuberculosis detection. Expert Rev Mol Diagn 17: 427-443, 2017.
130. Li M, Singh R, Wang Y, Marques C, Zhang B and Kumar S: Advances in novel nanomaterial-based optical fiber biosensors-a review. Biosensors (Basel) 12: 843, 2022.
131. Vu CQ and Arai S: Quantitative imaging of genetically encoded fluorescence lifetime biosensors. Biosensors (Basel) 13: 939, 2023.
132. Hemmerová E and Homola J: Combining plasmonic and electrochemical biosensing methods. Biosens Bioelectron 251: 116098, 2024.